Drug Design, Development and Therapy

Dovepress

open access to scientific and medical research

Open Access Full Text Article

ORIGINAL RESEARCH

Gancao Xiexin Decoction Ameliorates Ulcerative Colitis in Mice via Modulating Gut Microbiota and Metabolites

Yi-ting Luo[1], Jin Wu[1], Fang-yuan Zhu[1], Jia-qian Wu[1], Pei Wu[1], Ying-chao Liu[2]

[1]The Second Clinical Medical College, Zhejiang Chinese Medical University, Hangzhou, People's Republic of China; [2]Academic Affairs Office, Zhejiang Chinese Medical University, Hangzhou, People's Republic of China

Correspondence: Ying-chao Liu, Zhejiang Chinese Medical University, 548 Binwen Road, Hangzhou, 310053, People's Republic of China, Tel +86-057318661190, Email jcjsylyc@163.com

Purpose: Ulcerative colitis (UC) is a chronic inflammatory bowel disease that starts with mucosal inflammation of the rectum and extends proximally in the colon in a continuous manner over a variable distance. Although it is more common in North America and Western Europe, its incidence is also increasing in Asia. Despite the introduction of several different classes of medications, the treatment options for UC may be insufficiently effective and burdened with significant side effects. In the present study, the therapeutic effects of Gancao Xiexin decoction (GCXX) were investigated on mice with dextran sulfate sodium (DSS)-induced colitis with exploration of the underlying mechanisms.

Methods: Colitis was induced in C57BL/6 mice by administering 3% DSS in drinking water for 7 days. GCXX and (or) the standard of care anti-inflammatory drug, mesalazine (5-aminosalicylic acid) were then administered for 7 days. The gut microbiota was characterized by 16S rDNA high-throughput gene sequencing and gut metabolites were detected by untargeted metabolomics. Germ-free mice were subsequently used to determine whether GCXX ameliorated UC principally through modulation of the gut microbiota.

Results: GCXX treatment was demonstrated to significantly reduce disease activity index (DAI) scores, prevent colonic shortening, ameliorate colonic tissue damage and reduce the levels of pro-inflammatory cytokines. Furthermore, analysis of the gut microbiota showed that GCXX-treated mice had higher relative quantity of *Dubosiella* ($P<0.05$) and lower relative quantity of *Escherichia-Shigella* ($P<0.05$). Metabolomics analysis indicated that GCXX could reduce the level of linoleic acid ($P<0.05$) and regulate its metabolism pathway. Moreover, in germ-free mice, GCXX failed to increase body weight, reduce DAI scores, or alleviate either colonic shortening or colonic damage.

Conclusion: The present study demonstrated that GCXX ameliorated DSS-induced colitis principally through modulating the gut microbiota and metabolites. This information should be integrated into the overall mechanisms of GCXX treatment of UC.

Keywords: gancao xiexin decoction, ulcerative colitis, gut microbiota, metabolomics, germ-free mice, *dubosiella*, *Escherichia-Shigella*, linoleic acid

Introduction

Ulcerative colitis (UC) is the most prominent subtype of inflammatory bowel diseases (IBD), which is characterized by chronic mucosal inflammation starting in the rectum and extending proximally in a continuous manner for a variable distance. It manifests as abdominal pain, bloody stool, and chronic diarrhea, with colonic biopsies demonstrating chronic inflammation.[1,2] Although the etiology of UC has yet to be fully clarified, it is complex and appears multifactorial with most investigators citing genetic susceptibility, defective immune response, mucosal barrier damage, and an imbalance of gut microbiota.[3–5]

In recent years, the gut microbiota has been recognized as playing an important role in the development and progression of UC. Studies have reported that structurally, the gut microbiota in UC patients was altered when compared with healthy people, such as a decrease of the quantity and diversity of gut microbiota; of particular note has been the

Received: 11 December 2021
Accepted: 25 April 2022
Published: 9 May 2022

ratio of the two most important bacterial phyla in the gastrointestinal tract, specifically a decrease of Firmicutes and an increase of Bacteroidetes.[6–8] Additionally, mounting evidence has indicated that metabolites produced by the gut microbiota could also influence the development of UC, and that disorders in metabolism have been common in UC patients. Reportedly, this included an imbalance of short chain fatty acids (SCFAs)[9,10] that can induce intestinal epithelial cells to secrete interleukin (IL)-18, which in turn can repair the epithelium, increase the integrity of epithelial cells, and promote the production of goblet cell mucin and modify the tight junctions.[11–13]

Epidemiologic studies have estimated that the overall incidence of IBD was 5–15 per 100,000 person years in the Western world, affecting over 2 million individuals in North America, 3.2 million in Europe, and millions more worldwide.[14,15] This also includes an increasing incidence in Asia and in developing countries.[16–19] Therefore, continued emphasis is justified in pursuing additional treatment options for UC. At present, the drugs used to treat UC principally include aminosalicylates, steroids, immunosuppressants and biologics.[20,21] However, these drugs are not always successful, and often cause potentially significant side effects, such as infection, toxic effects and intolerance.[22] Thus, the search for new and effective treatments of UC has extended to traditional Chinese medicine (TCM). Gancao Xiexin decoction (GCXX), which is derived from Shanghan Lun, a Chinese medical archive written by Zhang Zhongjing (150–219 CE), is a well-known classical prescription used in treating Behcet's disease and has also been used by Chinese herbal doctors to treat UC for many years.[23] The formula for GCXX includes seven herbs: Gan Cao (Glycyrrhiza uralensis), Gan Jiang (Rhizoma zingiberis), Ban Xia (Pinellia), Huang Qin (Scutellaria baicalensis), Dang Shen (Codonopsis radix), Da Zao (Ziziphus jujube) and Huang Lian (Coptis). One report found that, compared with mesalazine, GCXX relieved or eliminated clinical symptoms, improved pathological changes of the colon, and had both a higher cure rate and lower recurrence rate.[24] GCXX was also found to decrease serum levels of IL-6, IL-17 and tumour necrosis factor (TNF)-α, increase blood levels of $CD8^+$, and reduce the ratio of $CD4^+/CD8^+$ in UC patients.[25] Using real-time polymerase chain reaction (RT-PCR) technology to detect the specific bacterial content in the intestines of UC patients comparing pre- and post-GCXX treatment, the quantity of *Bifidobacteria* and *Lactobacilli* increased whereas E. coli decreased.[26] Although these studies found that GCXX could regulate gut microbiota in UC patients, the mechanisms of the modifications of the gut microbiota structure and metabolites have not been reported. Therefore, the aims of this study were to investigate the mechanisms and therapeutic effects of GCXX on the alterations of the gut microbiota and metabolites in patients with UC.

A well-established murine model of UC was initially induced by dextran sulfate sodium (DSS).[27–29] To provide proof of the UC-murine model and assess the therapeutic efficacy of GCXX, the body weight, colon length, disease activity index (DAI) score, histopathological score of the colon and serum inflammatory cytokines were measured. UC was treated with either mesalazine alone or in combination with GCXX, and changes of the gut microbiota were detected by 16S rDNA high-throughput gene sequencing. Ultra-performance liquid chromatography combined with quadrupole time-of-flight mass spectrometry (UPLC-Q-TOF-MS)-based untargeted metabolomics was applied to analyze the metabolite profiles derived from gut microbiota, and to monitor and capture potential metabolic responses and biomarkers. Finally, we used germ-free mice to further determine whether the amelioration of UC was achieved principally through modulation of the gut microbiota. Therefore, the study aims were refined to identify the changes of key bacteria or metabolites that might provide new insight into the mechanism of GCXX treatment of UC as the scientific basis for its clinical application.

Materials and Methods

Chemicals and Reagents

Mesalazine was purchased from Shanghai Haoyuan Biomedical Technology Co., Ltd. (Shanghai, China); dextran sulfate sodium (DSS) was bought from MP Biomedicals (Santa Ana, CA, USA); methanol and acetonitrile were purchased from CNW Technologies (Shanghai, China); 2-chloro-L-phenylalanine was purchased from Shanghai Hengbai Biotech Co., Ltd. (Shanghai, China); formic acid was purchased from Sigma-Aldrich (St. Louis, MO, USA); enzyme-linked immunosorbent assay kits were purchased from Nanjing Jiancheng Bioengineering Institute (Nanjing, Jiangsu, China).

Preparation of GCXX

GCXX is comprised of 12 g of Gan Cao (Glycyrrhiza uralensis); 9 g of Gan Jiang (Rhizoma zingiberis), Ban Xia (Pinellia), Huang Qin (Scutellaria baicalensis), and Dang Shen (Codonopsis radix); 6 g of Da Zao (Ziziphus jujube); 3 g of Huang Lian (Coptis). All herbs were purchased from the Hangzhou Binjiang Chinese Medicine Clinic of Zhejiang Chinese Medical University (Hangzhou, Zhejiang, China) and were accredited by a pharmacologist. The dosage of GCXX was determined according to the clinical equivalent dose of experimental mice. The clinical daily dosage of GCXX for a human is 57 g (the total raw herbs). Equivalently, the dosage for mice was 8.55 g/kg/day, calculated by the formula that converts human dosage into that of mice according to the equivalent body surface area (Methodology on Chinese Medicinal Pharmacology).[30] An adult human body weight was estimated at 60 kg, mouse weight was estimated at 20 g; the conversion factor for the adult dose for mice was 9 (Wang et al also used this method).[31] Decoction was soaked with distilled water for 30 min, decocted for 30 min. Then, the medicines were concentrated to a final concentration of 1.7 g/mL. A portion of the GCXX liquid was stored at −80°C for UPLC-Q-TOF-MS analysis.

UPLC-Q-TOF-MS Analysis for GCXX

The samples of GCXX were thawed in ice water, vortexed for 30s and centrifuged at 12,000 rpm at 4°C for 10 min. A 300 μL aliquot of each individual sample was precisely transferred to an Eppendorf tube. After the addition of 1000 μL of extracting solution (methanol: water = 4:1, v/v, including internal standard (IS) at a ratio of 1000:10), all samples were vortexed for 30s, sonicated for 10 min in an ice-water bath, incubated at −80 °C for 1 h, and centrifuged at 12,000 rpm at 4°C for 10 min. A 400 μL aliquot of the supernatant was passed through a 0.22 μm filter membrane then transferred to an auto-sampler vial for UPLC-Q-TOF-MS analysis, which was performed on a Agilent ultra-high performance liquid chromatography 1290 UPLC system with a UPLC BEH C18 column (2.1 × 100 mm, 1.7 μm, Waters, UK). The flow rate was set at 0.4 mL/min and the sample injection volume was set at 5 μL. The mobile phase consisted of 0.1% formic acid in water (A) and 0.1% formic acid in acetonitrile (B). The multi-step linear elution gradient program was as follows: 0–3.5 min, 95–85% A; 3.5–6 min, 85–70% A; 6–6.5 min, 70–70% A; 6.5–12 min, 70–30% A; 12–12.5 min, 30–30% A; 12.5–18 min, 30–0% A; 18–25 min, 0–0% A; 25–26 min, 0–95% A; 26–30 min, 95–95% A. A Q Exactive Focus mass spectrometer coupled with Xcalibur software was employed to obtain the MS and MS/MS data based on the IDA acquisition mode. During each acquisition cycle, the mass range was from 100 to 1500, and the top three of every cycle were screened and the corresponding MS/MS data were further acquired. Sheath gas flow rate: 45 Arb, Aux gas flow rate: 15 Arb, Capillary temperature: 400°C, Full ms resolution: 70,000, MS/MS resolution: 17,500, Collision energy: 15/30/45 in NCE mode, Spray Voltage: 4.0 kV (positive) or −3.6 kV (negative).[32]

Animals

Specific-pathogen-free (SPF)-grade male C57BL/6 mice (6–8 weeks, 20–22 g) were purchased from Shanghai Slack Laboratory Animal Co., Ltd. (No. SCXK 2017–0005, Shanghai, China). The mice were raised in the Animal Experiment Center of Zhejiang Chinese Medical University and housed under a temperature of 22 ± 2°C and a standard 12 h light/dark cycle. The mice were allowed free access to standard chow and sterilized water. All experiments involving mice were approved by the Experimental Animal Ethics Committee of Zhejiang Chinese Medical University (IACUC-20191028-04), and all animal experiments also took place there. Animal welfare was carried out in strict accordance with the "Guidelines for the Management and Use of Laboratory Animals" (Ministry of Science and Technology, China, 2016)

Induction of UC and Treatment

After the 7-day adaptation period, C57BL/6 mice were randomly divided into five groups (ten mice in each group), named as normal-control (NC), UC model (UC), GCXX treatment (GCXX), mesalazine treatment (Mes) group, and GCXX combined with mesalazine treatment (GMes) group. The UC mice model was induced using 3% (w/w) DSS solution instead of distilled water as drinking water for 7 days.[27–29] Then mice in the GCXX group received 8.55 g/kg GCXX once daily, the Mes group received 200 mg/kg mesalazine, and the GMes group received 8.55 g/kg GCXX and

200 mg/kg mesalazine.[33,34] The mice of the NC and UC groups received an equal volume of distilled water. All mice were treated for 7 days by gastric gavage once a day.

Disease Activity Index (DAI)

The body weight, fecal consistency and fecal blood levels of mice in each group were recorded daily, and the DAI score was performed according to a previous report,[35] which was the sum of the percentage of weight loss, the stool consistency and rectal bleeding (details, Table 1).

Sample Collection and Preparation

Following 7 days of treatment, fresh stool samples were collected into frozen pipes and stored at −80°C. The blood of the mice was collected, centrifuged at 4°C, 3000 rpm for 10 min, and the serum was collected and stored at −80°C. The mice were euthanized using CO_2 and the length of colons were measured and photographed. The colons were cut into pieces, one piece of the colon tissues was fixed in 4% paraformaldehyde, the remaining colon tissues were stored at −80°C for later use.

Histopathological Analysis

The colon tissues were fixed in 4% paraformaldehyde, embedded in paraffin, stained with Hematoxylin and Eosin (H&E), and examined under light microscopy. The histopathological scores were calculated according to the damage of epithelial mucosa and inflammatory infiltration (details, Table 2).[36]

Enzyme-Linked Immunosorbent Assay (ELISA)

The collected serum samples were allowed to thaw at room temperature, then tested for TNF-α and IL-6 according to the ELISA kit instructions; each sample had 3 replicate wells. The absorbance of samples in each well was measured with a multifunctional microplate reader at a wavelength of 450 nm.

Table 1 Criteria for Disease Activity Index

Weight Loss (%)	Stool Consistency	Rectal Bleeding	Score
None	Normal	Occult blood test negative	0
1–5	Formed feces but easily adhere	Weak positive detection of occult blood	1
5–10	Semi-formed/soft feces	Occult blood test positive	2
10–20	Slurry stool but not adherent to the anus	Occult blood test strong positive	3
>20	Diarrhea and adherence to the anus	Gross bleeding	4

Table 2 Evaluation of Pathological Score

Epithelial Cells	Inflammatory Cell Infiltration	Score
Normal form	No infiltration	0
Goblet cell loss	Infiltration in basal layer of crypt	1
Large area loss of goblet cells	Infiltration reaches the mucosal muscle layer	2
Crypt cells loss	Infiltration deep into the mucosal muscle layer, accompanied by mucosal thickening and edema	3
Large area loss of crypt cells	Infiltration to the submucosa	4

DNA Extraction and 16S rDNA Gene Sequencing

The E.Z.N.A.® Stool DNA Kit (Omega Bio-tek, Norcross, GA, USA) was used to extract intestinal microbial community genomic DNA (five samples from NC group, UC group, Mes group, GMes group and seven samples from GCXX group). The DNA extraction quality was detected by 1% agarose gel electrophoresis, and the DNA was quantified by NanoDrop 2000 UV-vis spectrophotometer (Thermo Scientific, Wilmington, USA). The hypervariable region V3-V4 of the bacterial 16S rDNA gene was amplified with primer pairs 341F (5'-CCTACGGGNGGCWGCAG-3') and 805R(5'-GACTACHVGGGTATCTAATCC-3') by an ABI GeneAmp® 9700 PCR thermocycler (ABI, CA, USA). The PCR mixtures contained Phusion Hot start flex 2X Master Mix 12.5 μL, Forward Primer 2.5 μL, Reverse Primer 2.5 μL, Template DNA 50 ng, and finally ddH_2O up to 25 μL. PCR reactions were performed in triplicate. The PCR amplification of 16S rDNA gene was performed as follows: initial denaturation at 98°C for 30s, followed by 30 cycles of denaturing at 98°C for 10s, annealing at 54°C for 30s and extension at 72°C for 45s, and single extension at 72°C for 10 min, and end at 4°C. The PCR products were confirmed with 2% agarose gel electrophoresis. The PCR products were purified by AMPure XT beads (Beckman Coulter Genomics, Danvers, MA, USA) and quantified by Qubit (Invitrogen, USA). The amplicon pools were prepared for sequencing and the size and quantity of the amplicon library were assessed on an Agilent 2100 Bioanalyzer (Agilent, USA) and with the Library Quantification Kit for Illumina (Kapa Biosciences, Woburn, MA, USA), respectively. The libraries were sequenced on the NovaSeq PE250 platform.

Untargeted Analysis by UPLC-Q-TOF-MS

Metabolite Extraction

The collected samples were thawed on ice, and metabolites were extracted with 50% methanol Buffer (five samples from NC group, UC group, Mes group, GMes group and seven samples from GCXX group). Briefly, a 20 μL sample was extracted with 120 μL of precooled 50% methanol, vortexed for 1 min, and incubated at room temperature for 10 min; the extraction mixture was then stored overnight at −20°C. After centrifugation at 4000 *g* for 20 min, the supernatants were transferred into new 96-well plates. The samples were stored at −80°C prior to the liquid chromatography combined with mass spectrometry (LC-MS) analysis. In addition, pooled Quality Control (QC) samples were also prepared by combining 10 μL of each extraction mixture.

Parameter of Mobile Phase and Mass Spectrometry (MS)

All samples were acquired by the LC-MS system followed machine orders. First, all chromatographic separations were performed using an UPLC system (SCIEX, UK). An ACQUITY UPLC T3 column (100 mm × 2.1 mm, 1.8 μm, Waters, UK) was used for the reversed phase separation. The column oven was maintained at 35°C. The flow rate was 0.4 mL/min and the mobile phase consisted of solvent A (water, 0.1% formic acid) and solvent B (Acetonitrile, 0.1% formic acid). Gradient elution conditions were set as follows: 0–0.5 min, 5% B; 0.5–7 min, 5% to 100% B; 7–8 min, 100% B; 8–8.1 min, 100% to 5% B; 8.1–10 min, 5% B. The injection volume for each sample was 4 μL.

A high-resolution tandem mass spectrometer TripleTOF5600plus (SCIEX, UK) was used to detect metabolites eluted from the column. The Q-TOF was operated in both positive and negative ion modes. The curtain gas was set at 30 pounds per square inch (PSI), ion source gas1 was set 60 PSI, ion source gas2 was set at 60 PSI, and an interface heater temperature was 650°C. For positive ion mode, the ionspray voltage floating was set at 5000V. For negative ion mode, the ionspray voltage floating was set at −4500V. The mass spectrometry data were acquired in information-dependent acquisition (IDA) mode. The TOF mass range was from 60 to 1200 Da. The survey scans were acquired in 150 ms and as many as 12 product ion scans were collected if exceeding a threshold of 100 counts per second (counts/s) and with a 1 +charge-state. Total cycle time was fixed to 0.56 s. Four time bins were summed for each scan at a pulser frequency value of 11 kHz through monitoring of the 40 GHz multichannel target-decoy competition (TDC) detector with four-anode /channel detection. Dynamic exclusion was set for 4 s. During the acquisition, the mass accuracy was calibrated every 20 samples. Furthermore, to evaluate the stability of the LC-MS during the whole acquisition, a quality control sample (pool of all samples) was acquired after every 10 samples.

Bioinformation Analysis

T-tests were conducted to detect differences in metabolite concentrations between the 2 phenotypes. The P value was adjusted for multiple tests using an FDR (Benjamini-Hochberg). Supervised Partial Least Squares Discriminant Analysis (PLS-DA) was conducted through metaX to discriminate the different variables between groups. The variable importance in the projection (VIP) value was calculated. A VIP cut-off value of 1.0 was used to select important features.

Induction of Germ-Free UC Mice

After the 7-day adaptation period, C57BL/6 mice were randomly divided into three groups (six mice in each group), named as normal-control (NC) group, germ-free UC model (GFUC) group, and GCXX treatment (GCXX) group. Mice in GFUC and GCXX groups were fed with antibiotic water for 5 days and then received 3% (w/w) DSS solution for 7 days. The antibiotic water contained 1 g/L ampicillin, 1 g/L metronidazole, 0.5 g/L vancomycin, and 0.5 g/L neomycin (according to Wu et al).[37] Then mice in the GCXX group received 8.55 g/kg GCXX once a day for 7 days. The mice of the NC and GFUC groups received an equal volume of distilled water.

Statistical Processing

SPSS software (version 25.0, SPSS Inc., Chicago, IL, USA) was used for data analysis. The normally distributed data were expressed as mean ± standard deviation (SD) and skewed data were presented as median (min - max). The Shapiro–Wilk test was used to assess data distribution. The ANOVA statistical test was performed to compare the data among multiple groups when the data was normally distributed, and was followed by the Least Significant Difference post-hoc test. The Kruskal–Wallis test was used when the data had a non-normal distribution, and was followed by Dunn's post hoc test. $P<0.05$ indicated that the difference was statistically significant.

Results

Component Analysis of GCXX

To identify the major chemical components, GCXX samples were analyzed by UPLC-Q-TOF-MS. The total positive (Figure 1A) and negative (Figure 1B) ion chromatograms of GCXX demonstrated the chemical composition of all compounds. Several components were found in GCXX. As shown in Figure 1C, 15 compounds were distinguished: 1) licoricesaponin G2, 2) isoliquiritin, 3) liquiritin, 4) isoliquiritigenin, 5) liquiritigenin, 6) curcumin, 7) wogonoside, 8) wogonin, 9) scutellarin, 10) astragaloside IV, 11) berberine, 12) epiberberine, 13) lobetyolin, 14) palmatine, and 15) jatrorrhizine. Three doses of GCXX had been tested, and the TIC maps of QC and the other two doses were shown in Supplement Figure 1.

Effect of GCXX on Activity, Food Intake, Body Weight, DAI Score, and Colon Length of Mice with DSS-Induced Colitis

Compared with the NC group, the activity, food intake and body weight of mice that received DSS were significantly decreased. Following administration of GCXX and (or) mesalazine, the activity and food intake of the mice were improved compared with mice without treatment, and although the body weight initially decreased, it then gradually increased. Following administration of the medication to the UC group, the body weight was significantly lower than in the NC, GCXX, Mes and GMes groups; there were no differences among the NC, GCXX, Mes and GMes group (Figures 2A and B).

Starting from the first day of inducing UC, the DAI scores were recorded daily. The DAI scores gradually increased in mice that received DSS. During administration of GCXX and (or) mesalazine, the DAI scores decreased gradually, and after the medication, the DAI scores of mice in the GCXX group, Mes group and GMes group were significantly lower than those in the UC group ($P<0.01$), and there were no differences among the GCXX, Mes and GMes groups (Figure 2C).

Furthermore, measurements of the colon length, as shown in Figure 2D, showed a reduction of approximately 24.7%, 10.8%, 7.3% and 10.4% in colon length in the UC, GCXX, Mes and GMes groups, compared with the NC group,

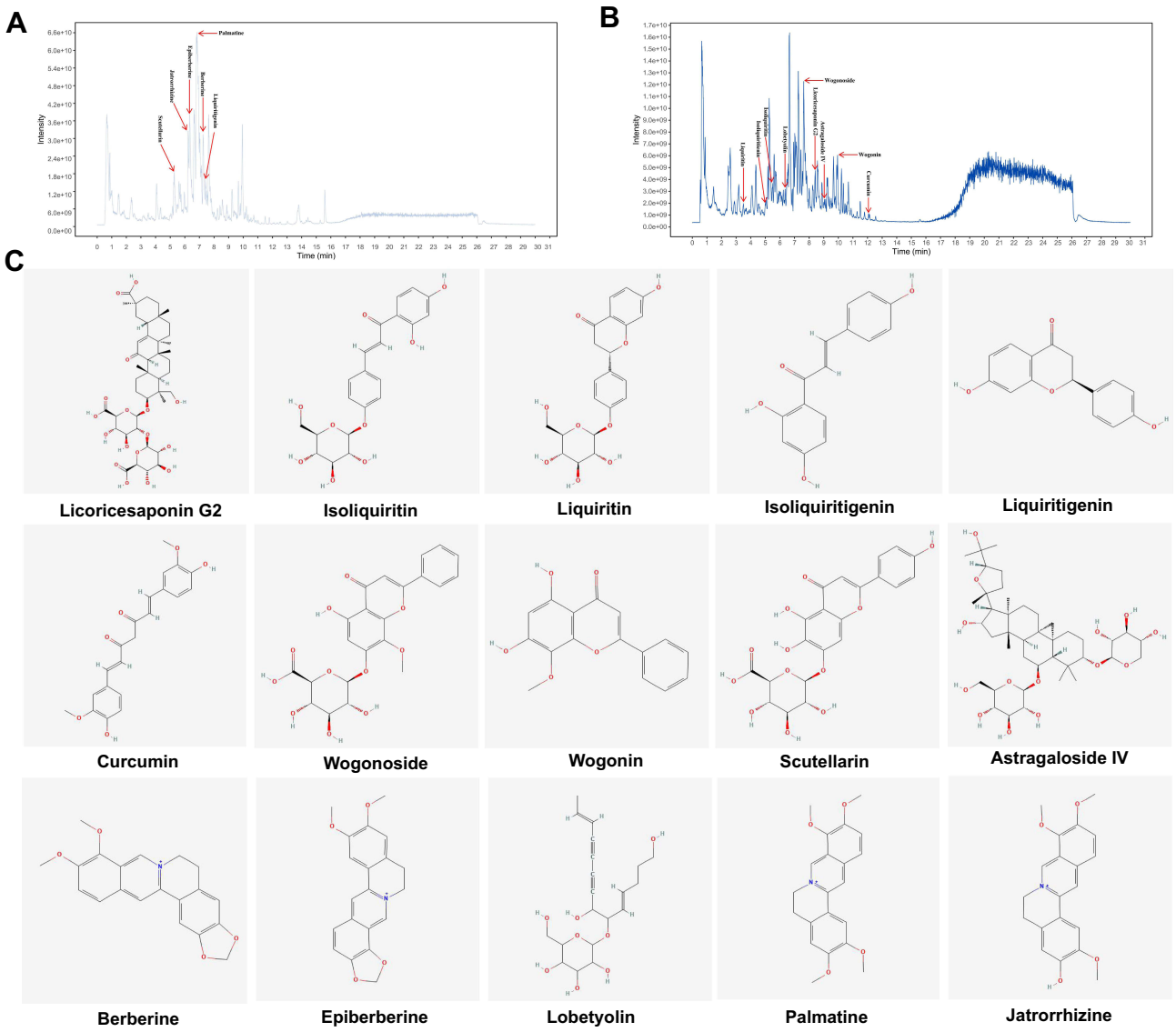

Figure 1 Identification of chemical components of GCXX. (**A**) Total ion chromatogram (TIC) in positive ion mode for GCXX samples; (**B**) TIC in negative ion mode for GCXX samples; (**C**) Molecular structure of constituents.

respectively. The colon length in the UC group was significantly shorter than in the NC group (P<0.001), GCXX group (P<0.01), Mes group (P<0.05) and GMes group (P<0.01); there were no differences among the NC, GCXX and GMes groups (Figure 2E).

GCXX Improved Mucosal Inflammation of Colonic Tissues

The typical histopathological manifestations of the colon in each group are shown in Figure 3A. The colon tissue of mice in the NC group showed completely in-tact colonic epithelium with small amounts of inflammatory cell infiltration. In contrast, in the UC group, there was obvious erosion and ulceration in the mucosal epithelium and considerable inflammatory cell infiltration in the lamina propria and submucosa. However, in the GCXX, Mes and GMes groups, the inflammatory infiltration and destruction of the intestinal wall were notably milder than those in the UC group.

The histopathological scores of colons from mice in the UC group were significantly higher than those in the NC group (P<0.001). The histopathological scores of the colon in the GCXX, Mes, and GMes groups were significantly

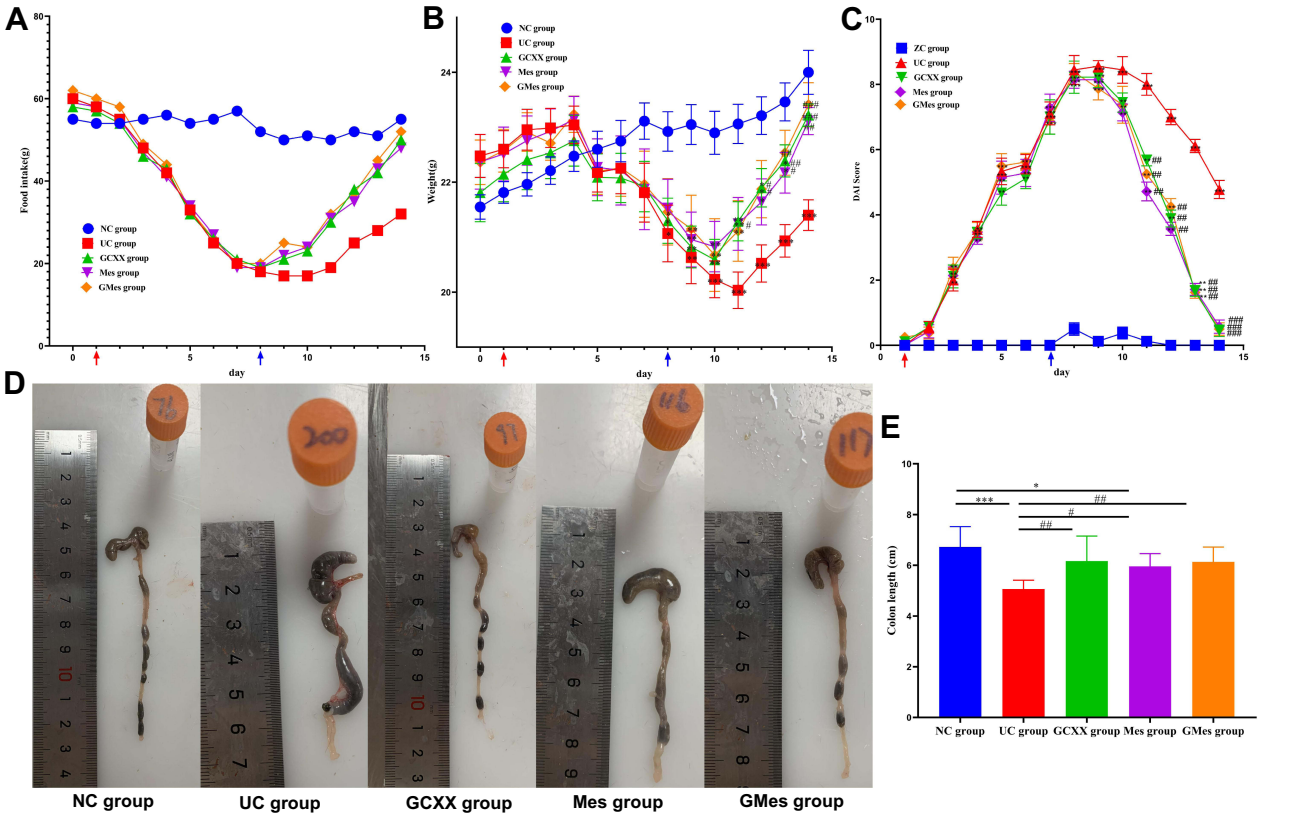

Figure 2 The food intake, body weight, DAI score and colon length of mice in each group. (**A**) Food intake of each group; (**B**) Changes in body weight of mice throughout the experiment; (**C**) Changes in DAI scores of mice throughout the experiment; (**D**) Typical colon anatomy of mice in each group; (**E**) The colon length of mice in each group. ***P<0.001, **P<0.01, *P<0.05. The red arrow means the first day of inducing UC by DSS and the blue arrow indicates the first day of medication. Compared with the NC group, ***P<0.001, **P<0.01, *P<0.05; compared with the UC group, ###P<0.001, ##P<0.01, #P<0.05.

lower than those from mice in the UC group (P<0.001). There were no differences among the GCXX, GMes and NC groups (P>0.05) (Figure 3B).

GCXX Regulated Cytokine Expression in Serum of Mice with DSS-Induced Colitis

Compared with the NC group, mice in the UC group exhibited increased serum levels of IL-6 and TNF-α (P<0.001). Following treatment with GCXX and (or) mesalazine, the serum levels of IL-6 and TNF-α decreased significantly from their high levels (P<0.001) but did not return completely back to the normal levels of the NC group (Figures 4A and B).

Effects of GCXX on Gut Microbiota Diversity

Rarefaction curves of observed operational taxonomic units (OTUs) tended to be flat with deepening of sequencing, which indicated that the depth of sequencing had covered all species in the sample, and sequencing of the gut microbiota was of good quality (Supplement Figure 2). The Venn diagram in Figure 5A shows that the five groups shared 229 OTUs, the NC and UC groups shared 457 OTUs, the NC and GCXX groups shared 581 OTUs, and the GCXX and UC groups shared 589 OTUs. In addition, 1570, 915, 1081, 893, 563 OTUs were uniquely presented in the NC, UC, GCXX, Mes and GMes groups, respectively.

To investigate the alpha diversity of the gut microbiota in each group, we used the Chao1 and Shannon indices. As shown in Figures 5B-E, the rarefaction curves of the two indices plateaued with the increase of sequence number. The results showed that compared with the NC group, the Chao1 index and Shannon index of the UC group decreased slightly, but the difference was not significant. This indicated that the alpha diversity of the gut microbiota of the UC group slightly changed after modeling. In addition, compared with the UC group, although the Chao1 and Shannon

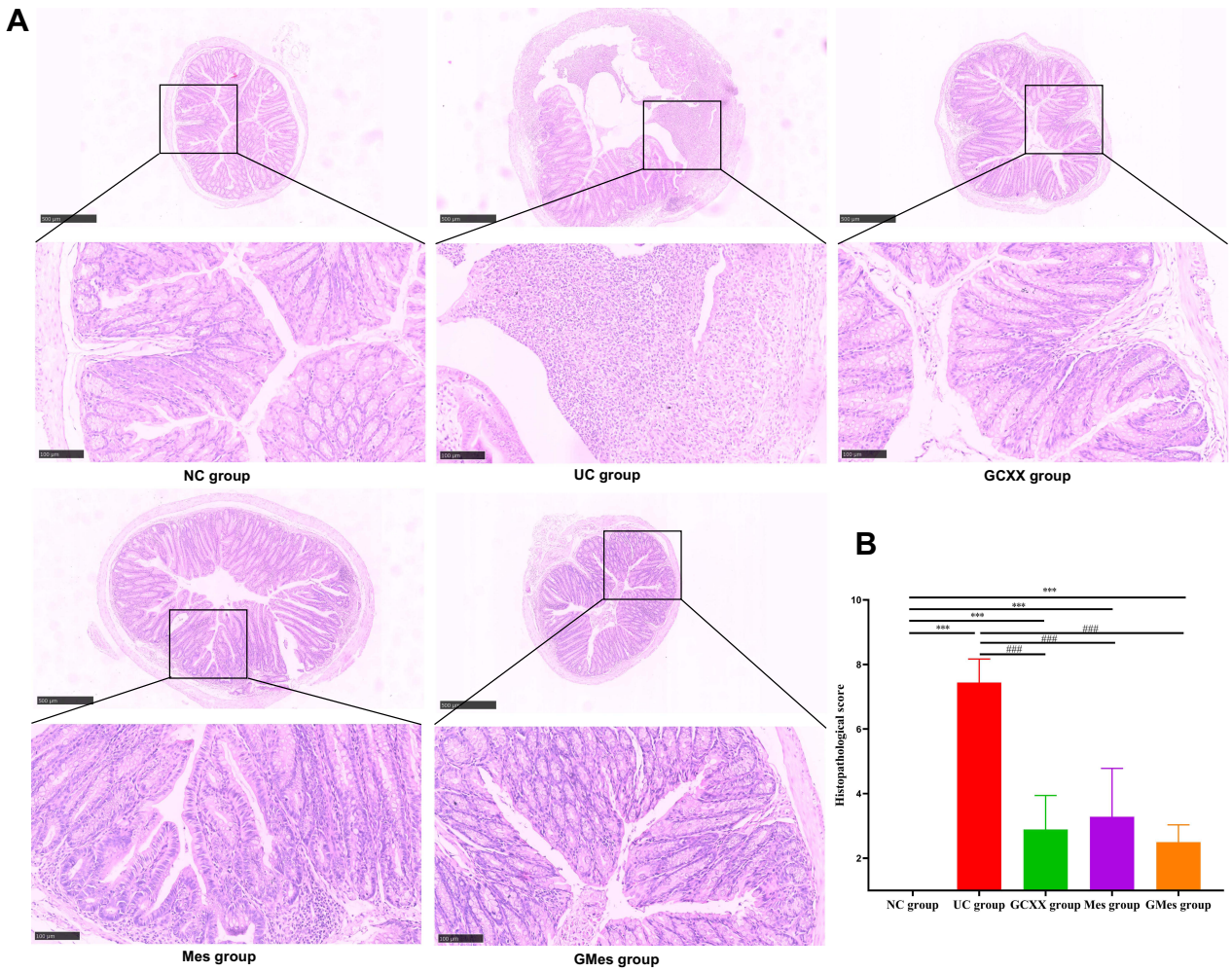

Figure 3 Histopathological changes and scores of colonic tissues of mice in each group. (**A**) Typical histopathological performance of each group (× 5 and × 20). (**B**) Histopathological score of each group. Compared with the NC group, ***P<0.001; compared with the UC group, ###P<0.001.

indices in the GCXX groups decreased slightly, the difference was not significant. However, unexpectedly, compared with the NC group, the Chao1 index in the GCXX, Mes and GMes groups significantly decreased ($p<0.05$, $p<0.05$, $p<0.05$).

To measure beta diversity of the gut microbiota in each group, we used principal coordinate analysis (PCoA) of unweighted UniFrac distances and Bray-Curtis dissimilarity. As shown in Figure 5F, the scatter plot of the NC group clearly deviated from the other four groups; this indicated that the composition of the gut microbiota had changed significantly after the model was established. Additionally, the scatter plot of the GCXX, GMes and the UC groups partially overlapped each other, which indicated that treatment could regulate abnormal changes of the gut microbiota. These results indicated that the gut microbiota of the UC group had dramatically changed in comparison to the NC group. Although GCXX treatment had improved the gut microbiota compared to the UC group, it did not fully restore it to normal when compared to the NC group.

Effects of GCXX on the Gut Microbiota Structure

To further understand the structure of the gut microbiota in UC mice and the effect of GCXX, the differences among groups at the level of phylum and species were analyzed. At the phylum level, 13 phyla were detected in all samples, and the dominant phyla in the NC group were Bacteroidetes, Firmicutes and Verrucomicrobia, with average relative proportions of 38.8%, 30.8% and 26.6%, respectively (stacked bar chart, Figure 6A). In the UC group, the

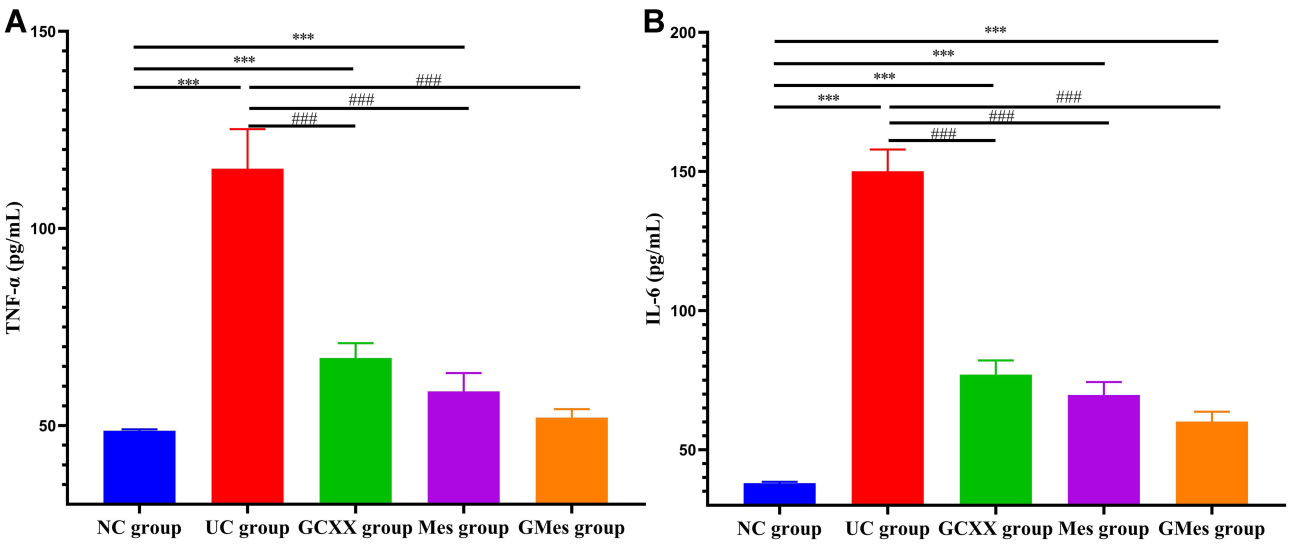

Figure 4 The levels of inflammatory cytokines in serum of mice in each group. (**A**) The levels of TNF-α in serum of mice; (**B**) The levels of IL-6 in serum of mice. Compared with the NC group, ***P<0.001; compared with the UC group, ###P<0.001.

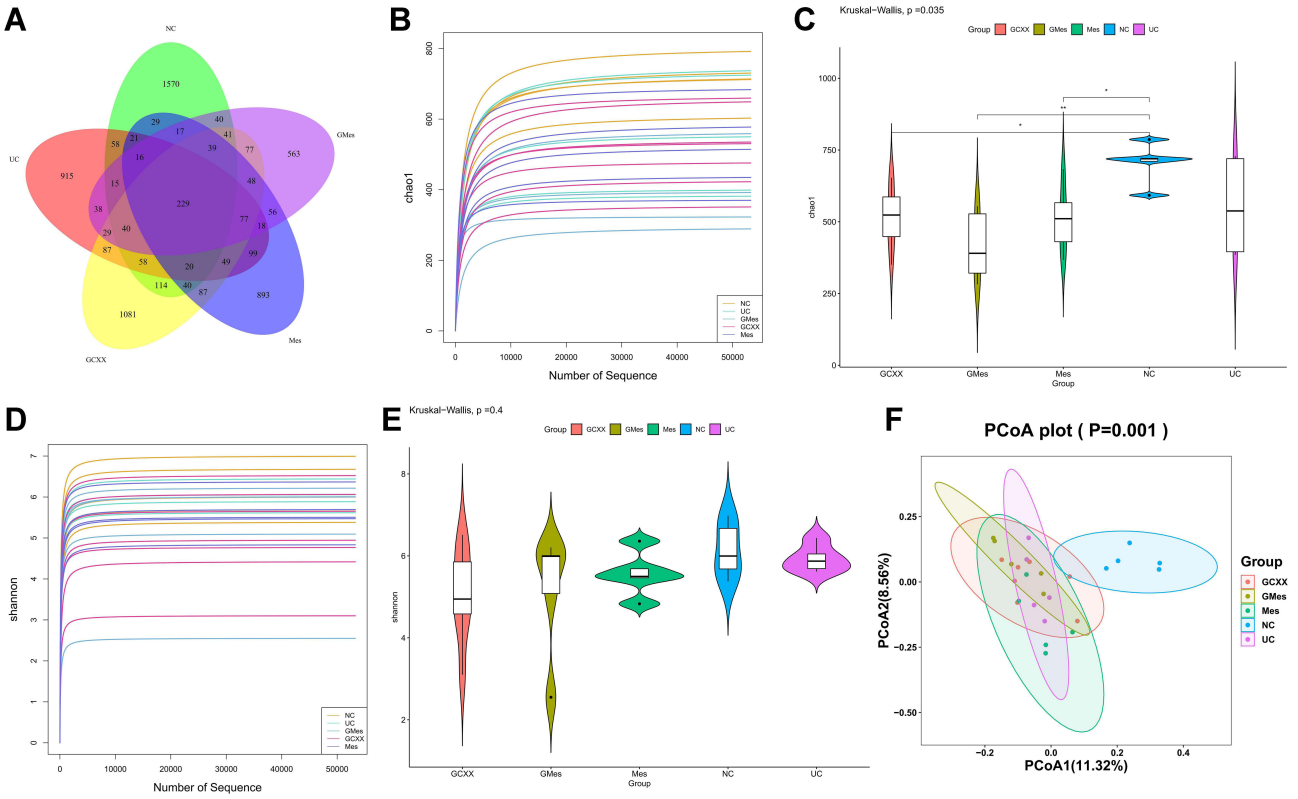

Figure 5 Effect of GCXX on gut microbiota diversity of mice in each group. (**A**) The Venn diagram indicated the differential numbers of OTUs in each group; (**B**) The rarefaction curves of Chao1 index; (**C**) The violin plot of Chao1 index; (**D**) The rarefaction curves of Shannon index; (**E**) The violin plot of Shannon index; (**F**) The PCoA plot of mice in each group. **P<0.01, *P<0.05.

proportion of Proteobacteria was significantly increased (P<0.05) and Patescibacteria significantly decreased (P<0.05) compared to those in the NC group. In addition, compared with the UC group, the proportion of Proteobacteria in the GCXX group was slightly decreased and the proportion of Patescibacteria was slightly increased, but neither difference was significant. At the genus level, the 30 most abundant bacterial genera were

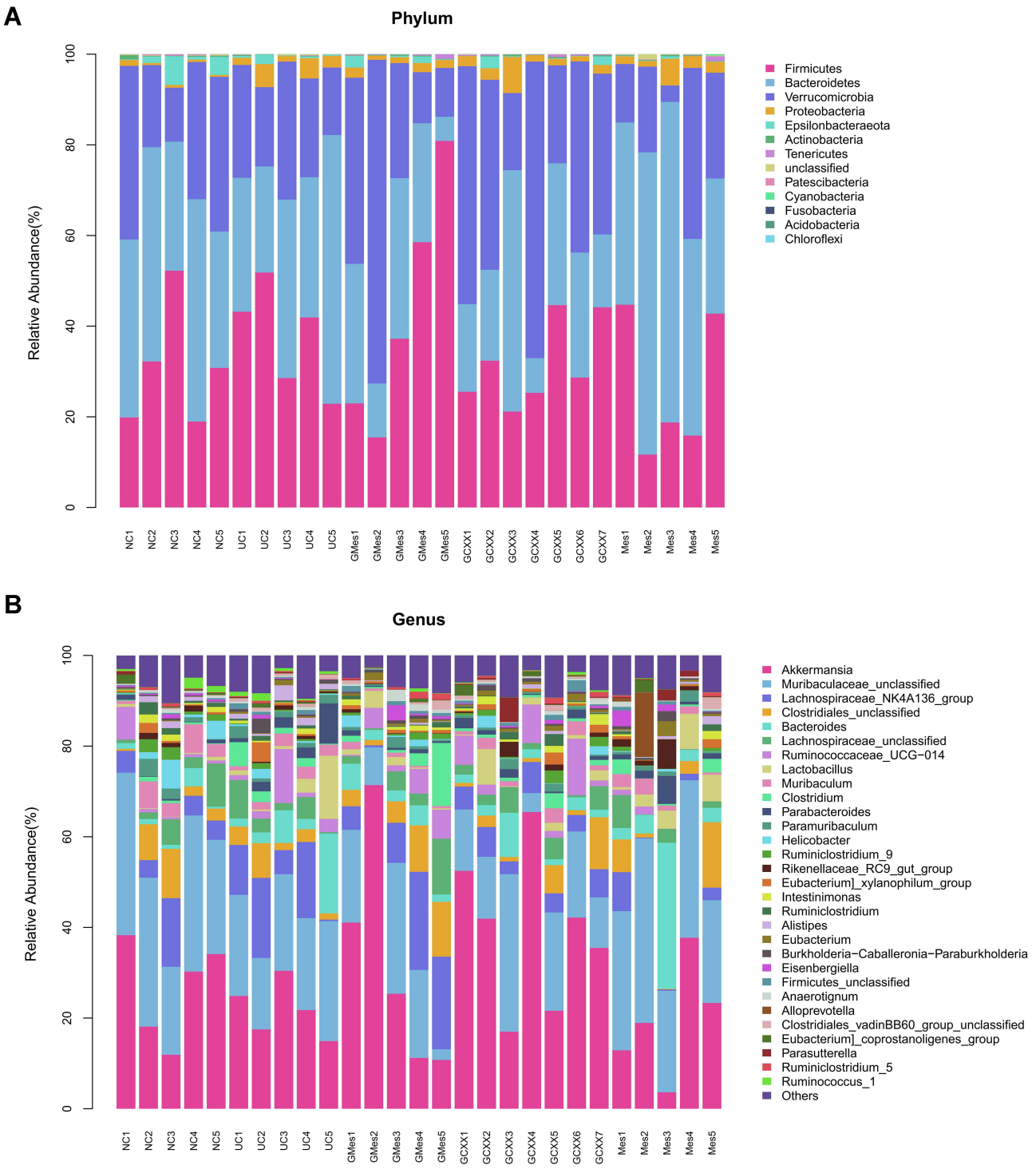

Figure 6 Effects of GCXX on the structure of gut microbiota. (**A**) The stacked bar chart of the structure of gut microbiota at the phylum level; (**B**) The stacked bar chart of the structure of gut microbiota at the genus level.

shown in the stacked bar chart, Figure 6B. In the NC group, *Muribaculaceae*_unclassified, *Akkermansia, Lachnospiraceae_NK4A136_group, Clostridiales*_unclassified, *Lachnospiraceae*_unclassified, *Muribaculum, Helicobacter, Ruminococcaceae_UCG-014, Ruminiclostridium_9* and *Bacteroides* were the top 10 most-abundant bacterial genera, with proportions ranging from 29.6 to 1.6%. In the UC group, the proportions of *Prevotellaceae_UCG-001, Dubosiella, Ureaplasma, Butyricicoccus, Angelakisella, Candidatus_Saccharimonas* and

several species from the *Eubacterium_brachy_group* decreased significantly compared to those in the NC group (all P<0.05). In contrast, the proportions of *Romboutsia, Eubacterium_nodatum_group, Ruminiclostridium_6, Clostridiales_vadinBB60_group*_unclassified, *Desulfovibrio, Escherichia-Shigella, Christensenellaceae*_unclassified, *Parabacteroides, Delftia, Turicibacter, Erysipelatoclostridium, Sphingomonadaceae*_unclassified, *Absiella, Anaerovorax, Bacteroides, Clostridium* and *Burkholderia-Caballeronia-Paraburkholderia* increased significantly (all P<0.05). Moreover, compared with UC group, the proportions of *Bilophila, Arsenophonus, Anaeroplasma, Ruminococcaceae_unclassified* and *Dubosiella* increased significantly in the GCXX group (all P<0.05), and the proportions of *Proteus, Peptococcus, Alistipes, Ruminococcus_1, Tyzzerella_3, Mycoplasma, Sphingomonas, Escherichia-Shigella* and *Ruminococcaceae_UCG-009* decreased significantly (all P<0.05)). Overall, the proportion of *Escherichia-Shigella* increased significantly (P<0.05) and *Dubosiella* decreased significantly (P<0.05) in the UC mice, whereas after intervention with GCXX, the proportion of *Escherichia-Shigella* decreased significantly (P<0.05) and *Dubosiella* increased significantly (P<0.05); importantly, there were no differences between the NC group and the GCXX group (Figures 7A-C).

To compare the composition of gut microbiota in each group, the linear discriminant analysis effect size (LEfSe) analysis was applied. Results revealed that the order Bifidobacteriales including the family Bifidobacteriaceae, the large class of Actinobacteria, within the order Bacteroidales the family Muribaculaceae, the family Prevotellaceae containing the genus *Prevotellaceae_UCG_001*; the genus *A2*, the genus *Angelakisella* and the genus *Dubosiella* were significantly enriched in the NC group. The genus *Alistipes*, the genus *Parabacteroides*, the family Tannerellaceae, the genus *Clostridiales_vadinBB60_group_unclassified*, the family Clostridiales_vadinBB60_group, the genus *Ruminiclostridium_6*, the genus *Sphingomonas*, the genus *Desulfovibrio*, the genus *Escherichia_Shigella*, the family Enterobacteriaceae, the order Enterobacteriales, the class Gammaproteobacteria and the phylum Proteobacteria were significantly enriched in the UC group. The genus *Eubacterium*, the family Eubacteriaceae, the family Desulfovibrionaceae, the order Desulfovibrionales and the class Deltaproteobacteria were significantly enriched in the GCXX group (Figure 8A). Linear discriminant analysis (LDA) was then used to estimate differential proportions of bacteria between the groups, and species with differential proportions between groups were identified based on LDA scores greater than 3 (details displayed in Figure 8B).

Effects of GCXX on Metabolism of Gut Microbiota

A highly sensitive and specific analytical method, UPLC-Q-TOF-MS was established and applied to identify the metabolic profiling of feces samples collected from the mice. Total ion chromatograms (TICs) and metabolite m/z-rt distribution maps were shown in Supplement Figures 3A-D. Principal component analysis (PCA) was used to distinguish the inherent trends within the metabolic data of each group. Figure 9A depicts the tendency for segregation of NC, UC, GCXX, Mes and GMes groups, suggesting significant variations in metabolites within the five groups. Additionally, the QC samples were clustered closely in PCA score plots, indicating the stability of the UPLC-Q-TOF-MS system throughout the whole analysis. Moreover, PLS-DA was used to force the classification of each component, facilitating the identification of similarities and differences between groups, and the validation plot supported the validity of this PLS-DA model (Figures 9B-E).

Metabolites with VIP scores >1 in the orthogonal partial least squares discriminant analysis (OPLS-DA) model and p<0.05 differences were considered potential metabolic biomarkers. The volcano plots showed the variables whose content differed between the groups being compared, illustrated in Figures 10A and B. There were 249 significantly differential abundant metabolites identified between the NC and UC groups, and 290 significantly differential abundant metabolites identified between the UC and GCXX groups. Heat maps were constructed to visually emphasize these significantly differentially abundant metabolites (Supplement Figures 4A and B). Specifically, the level of acetic acid significantly decreased in the DSS-induced colitis mice, and increased slightly with GCXX treatment, but did not return fully to normal levels. Additionally, compared with the NC group, the levels of glycine-tyrosine, phenylalanine-threonine and glutamic acid-phenylalanine decreased (p<0.05) in the UC group, and the levels of linoleic acid increased (p<0.05). After treatment with GCXX, these metabolites increased to normal levels (Figures 10C-F). Furthermore, the levels of L-tyrosine, tyrosine, L-threonine, glycyl-L-norleucine, serine, L-serine, pyruvic acid, glycyl-L-norleucine and glycine-tryptophan decreased in the DSS-induced colitis mice, and although they increased slightly following treatment with

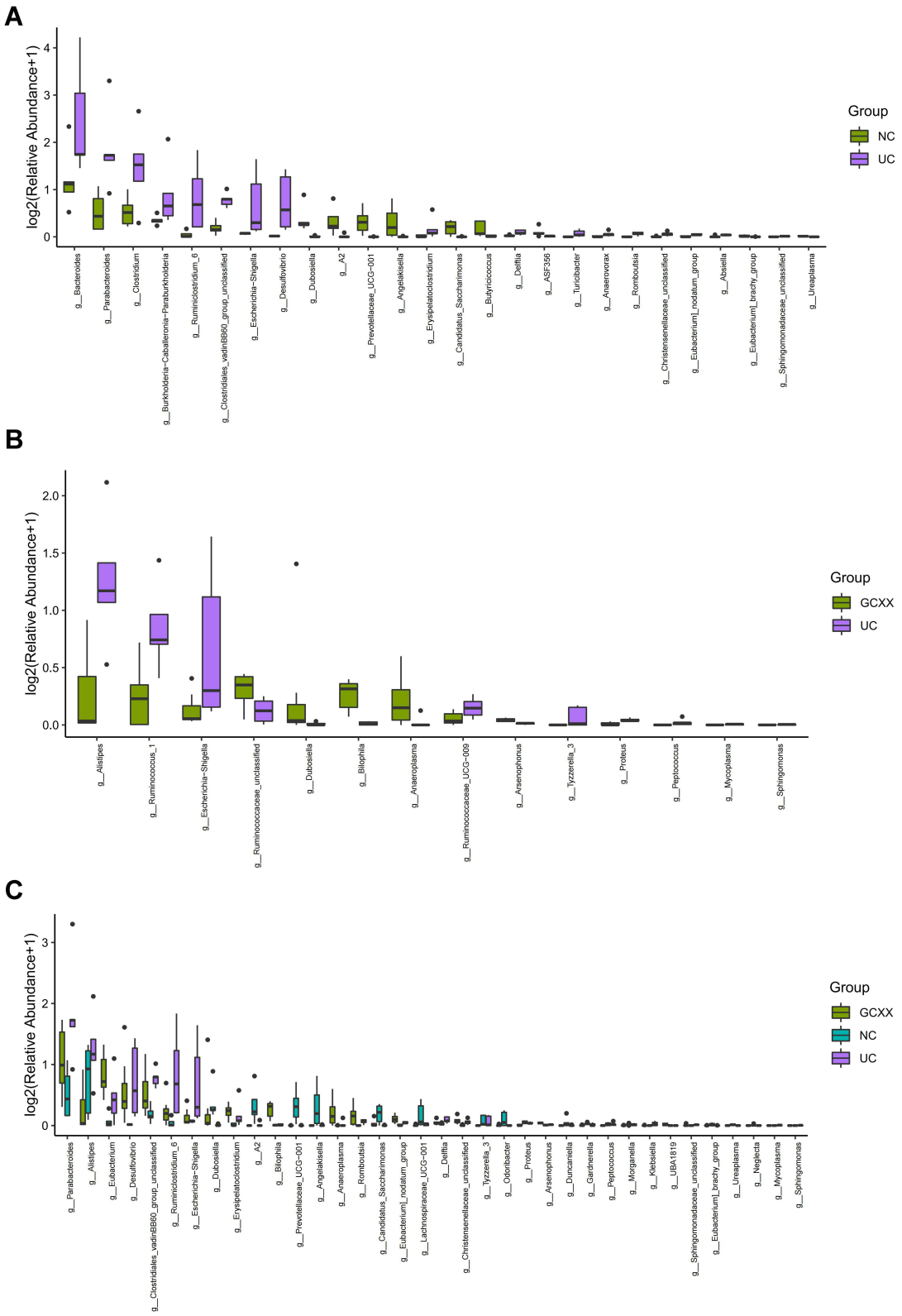

Figure 7 Gut microbiota at the genus level with significant differences among groups. (**A**) The difference boxplot of mice between NC group and UC group; (**B**) The difference boxplot of mice between GCXX group and UC group; (**C**) The difference boxplot of mice among ZC group, UC group and GCXX group.

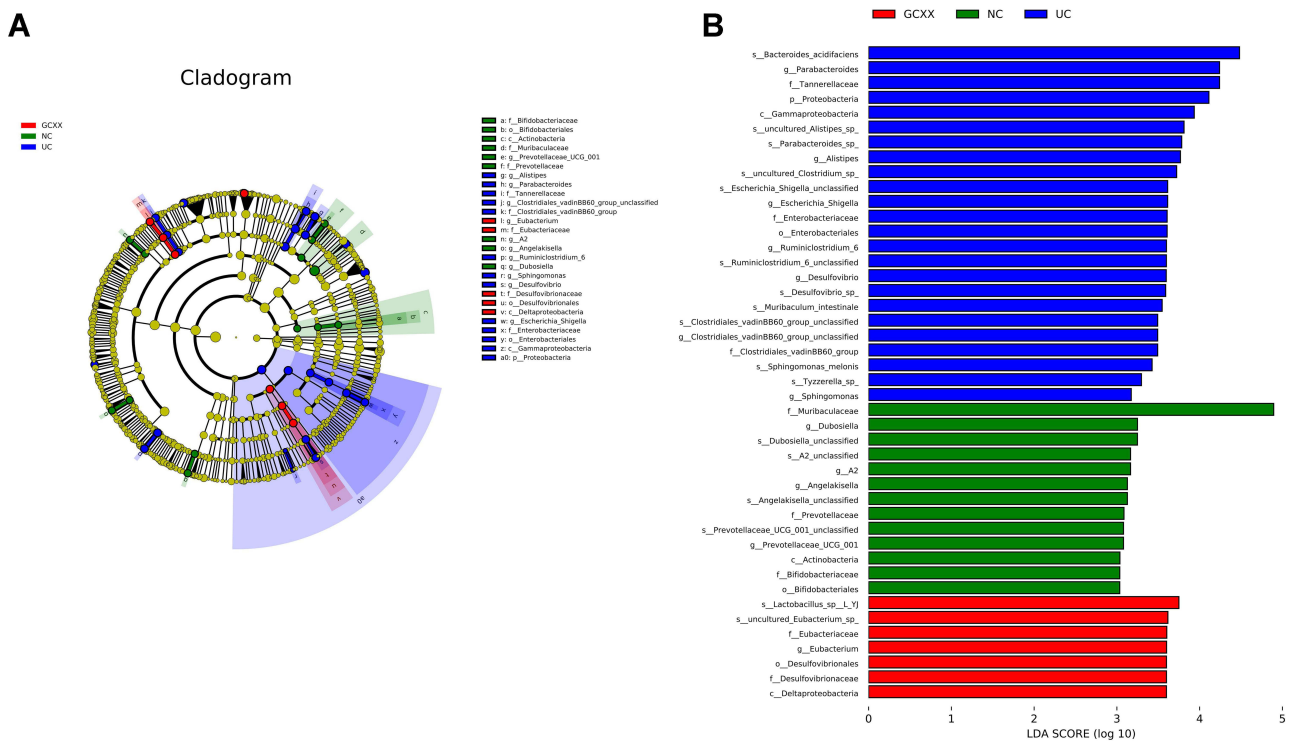

Figure 8 Annotation and difference analysis of gut microbiota structure. (**A**) LEfSe taxonomic cladogram of gut microbiota in each group; (**B**) LDA histogram in each group.

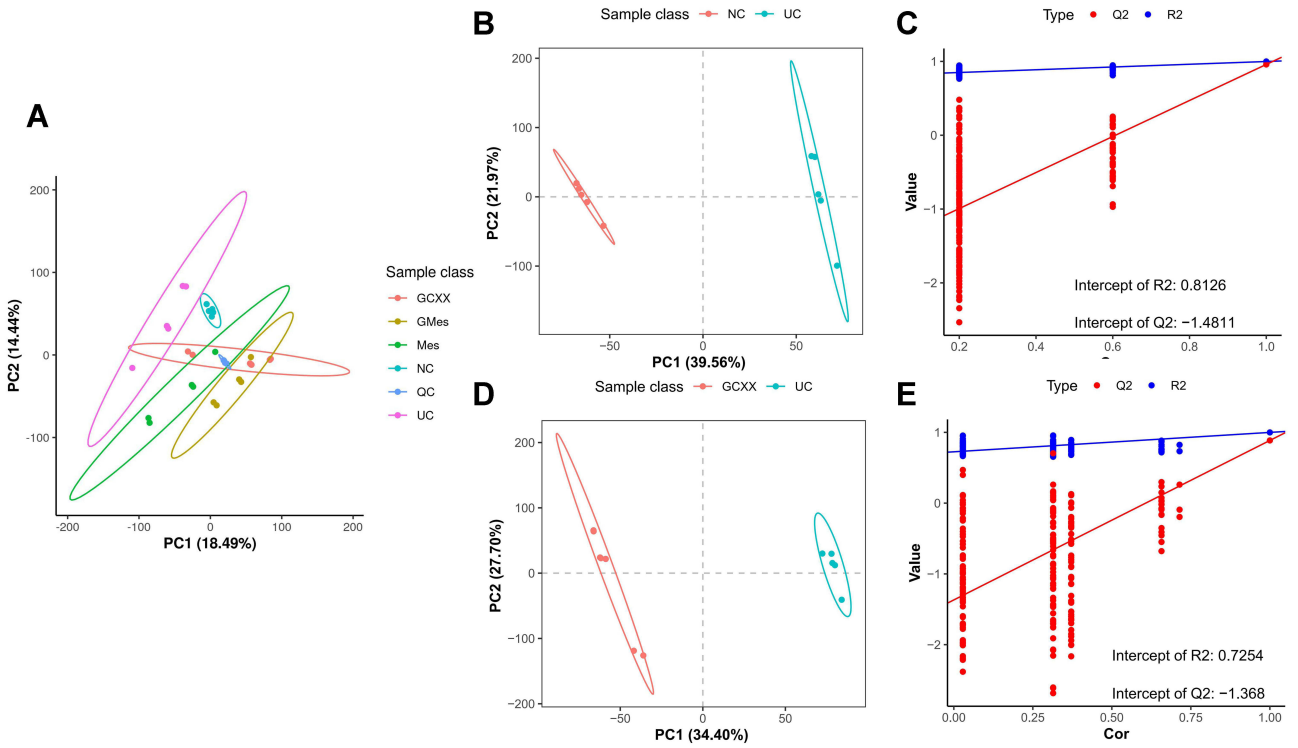

Figure 9 The Principal component analysis (PCA) and partial least squares discriminant analysis (PLS-DA) of mice in each group. (**A**) The PCA plot of mice in each group; (**B**) The PLS-DA plot between NC group and UC group; (**C**) The validation of PLS-DA model between NC group and UC group; (**D**) The PLS-DA plot between GCXX group and UC group; (**E**) The validation of PLS-DA model between GCXX group and UC group.

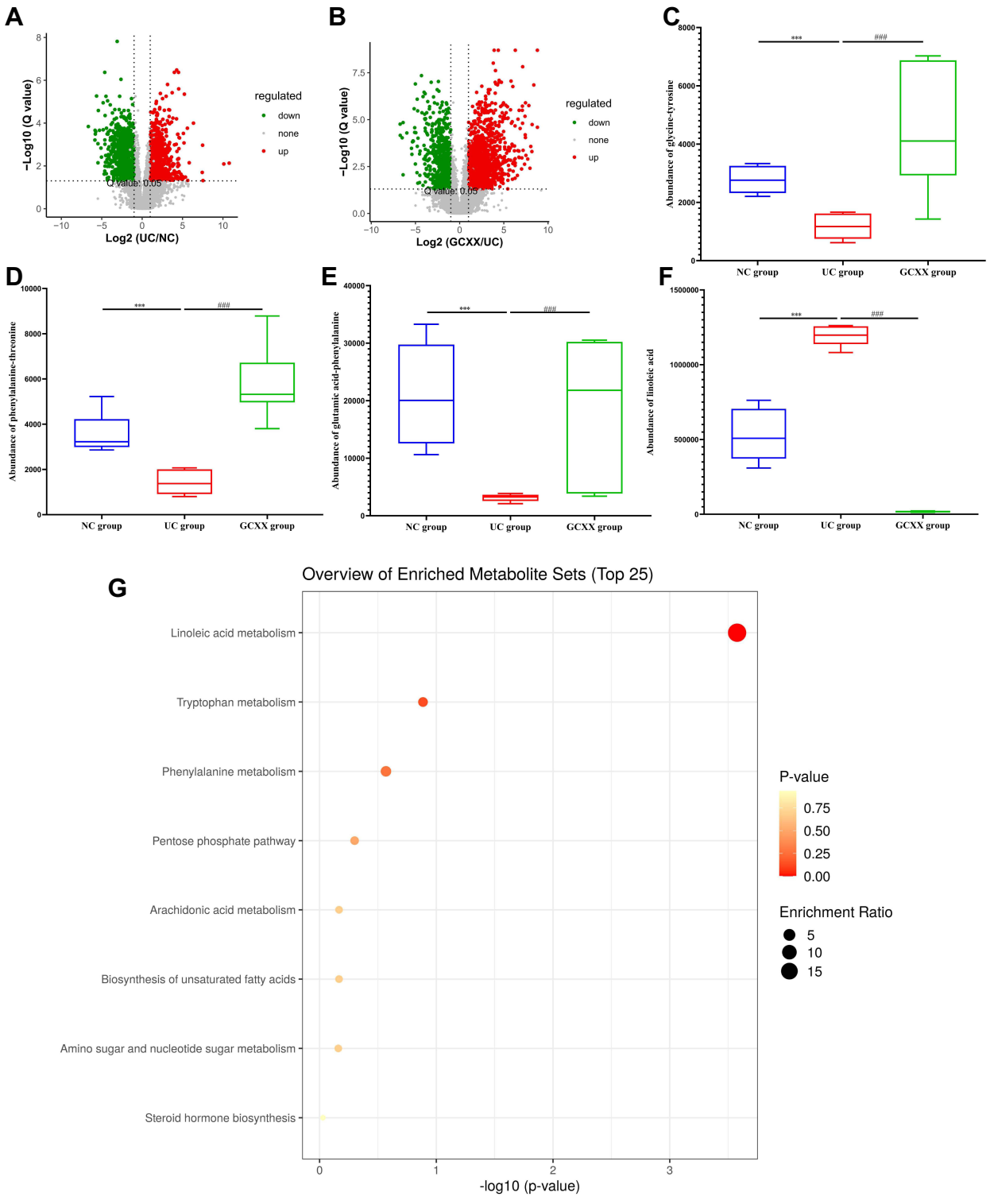

Figure 10 Continued.

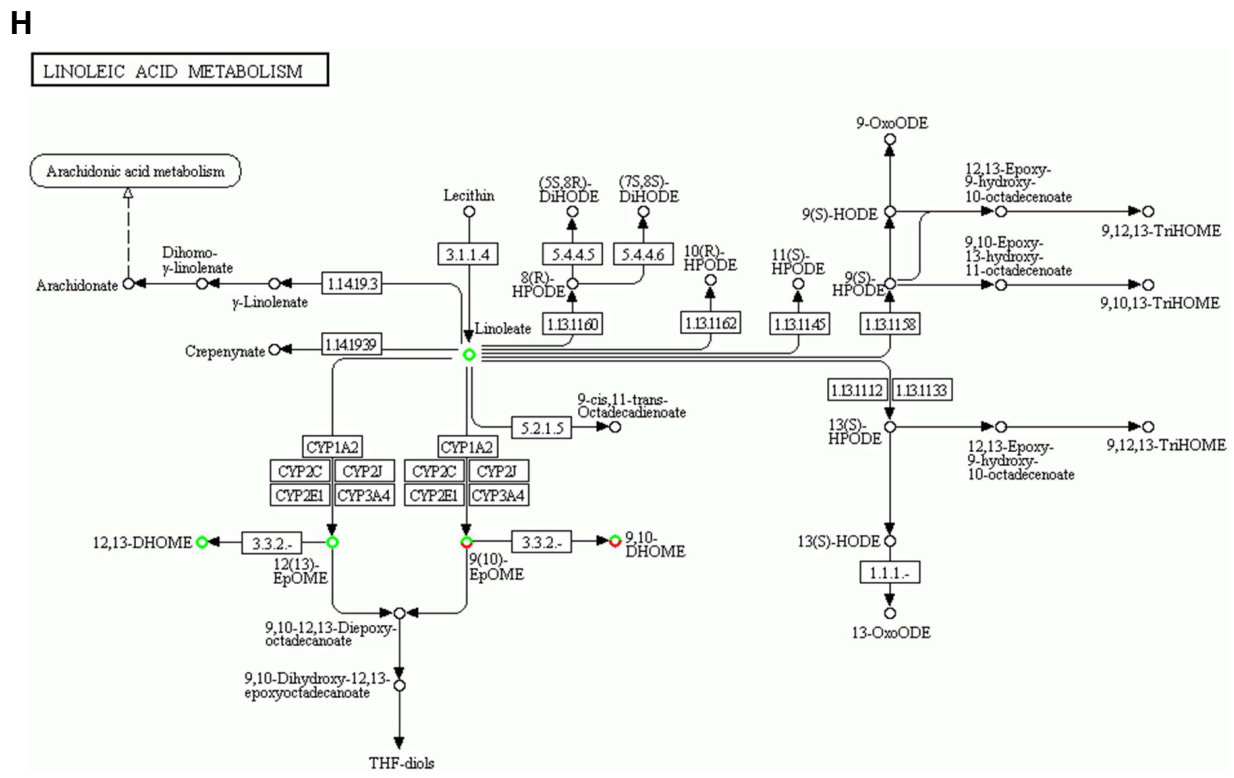

Figure 10 Effects of GCXX on metabolism of gut microbiota. (**A**) The volcano plot of mice between NC group and UC group; (**B**) The volcano plot of mice between GCXX group and UC group; (**C**) The abundance of glycine-tyrosine in each group; (**D**) The abundance of phenylalanine-threonine in each group; (**E**) The abundance of glutamic acid-phenylalanine in each group; (**F**) The abundance of linoleic acid in each group; (**G**) The bubble chart of differential metabolic pathways regulated by GCXX; (**H**) The pathway of linoleic acid metabolism. Red and green respectively indicate up-regulation and down-regulation of metabolites. Compared with the NC group, ***P<0.001; compared with the UC group, ####P<0.001.

GCXX, they did not return fully to normal levels. On further analysis, 39 metabolites significantly decreased following induction of UC, but intervention with GCXX resulted in significant increases in these metabolites such that there were no differences between the GCXX and NC groups. Moreover, there were 34 metabolites that significantly increased in the UC group compared to the NC group, but after using GCXX, these metabolites were significantly decreased and there were no differences between the GCXX and NC groups (Supplement Table S1).

Kyoto Encyclopedia of Genes and Genomes (KEGG) pathway enrichment analysis was undertaken to analyze 73 metabolites, and GCXX was found to be involved in the regulation of 8 metabolic pathways. The pathways included metabolic pathways of linoleic acid, tryptophan, phenylalanine, and arachidonic acid, as well as the pentose phosphate pathway, biosynthesis of unsaturated fatty acids, amino sugar and nucleotide sugar metabolism, and steroid hormone biosynthesis (Figure 10G). Specifically, GCXX principally regulated linoleic acid metabolism (P<0.05; Figure 10H).

Correlation Between the Gut Microbiota and Metabolites

To better understand the functional correlation between the gut microbiota and metabolites, the Pearson correlation analysis was carried out between the altered microbiota and perturbed metabolites. As shown in Figure 11, *Dubosiella* was negatively correlated with 7-Methylguanosine and positively correlated with quinaldic acid and tripelennamine. Moreover, *Escherichia-Shigella* was negatively correlated with 8 metabolites and was positively correlated with 39 metabolites.

GCXX Failed to Ameliorate DSS-Induced Colitis in Germ-Free Mice

For the final step in this investigation, we used germ-free mice to further determine whether the amelioration of UC using GCXX was primarily through modulation of the gut microbiota. In germ-free mice, we found that GCXX did not increase the body weight or reduce the DAI scores of the germ-free mice (Figures 12A and B). Furthermore, GCXX failed to alleviate colonic shortening (Figures 12C and D) or colonic damage (Figures 13A and B). These data seemed to

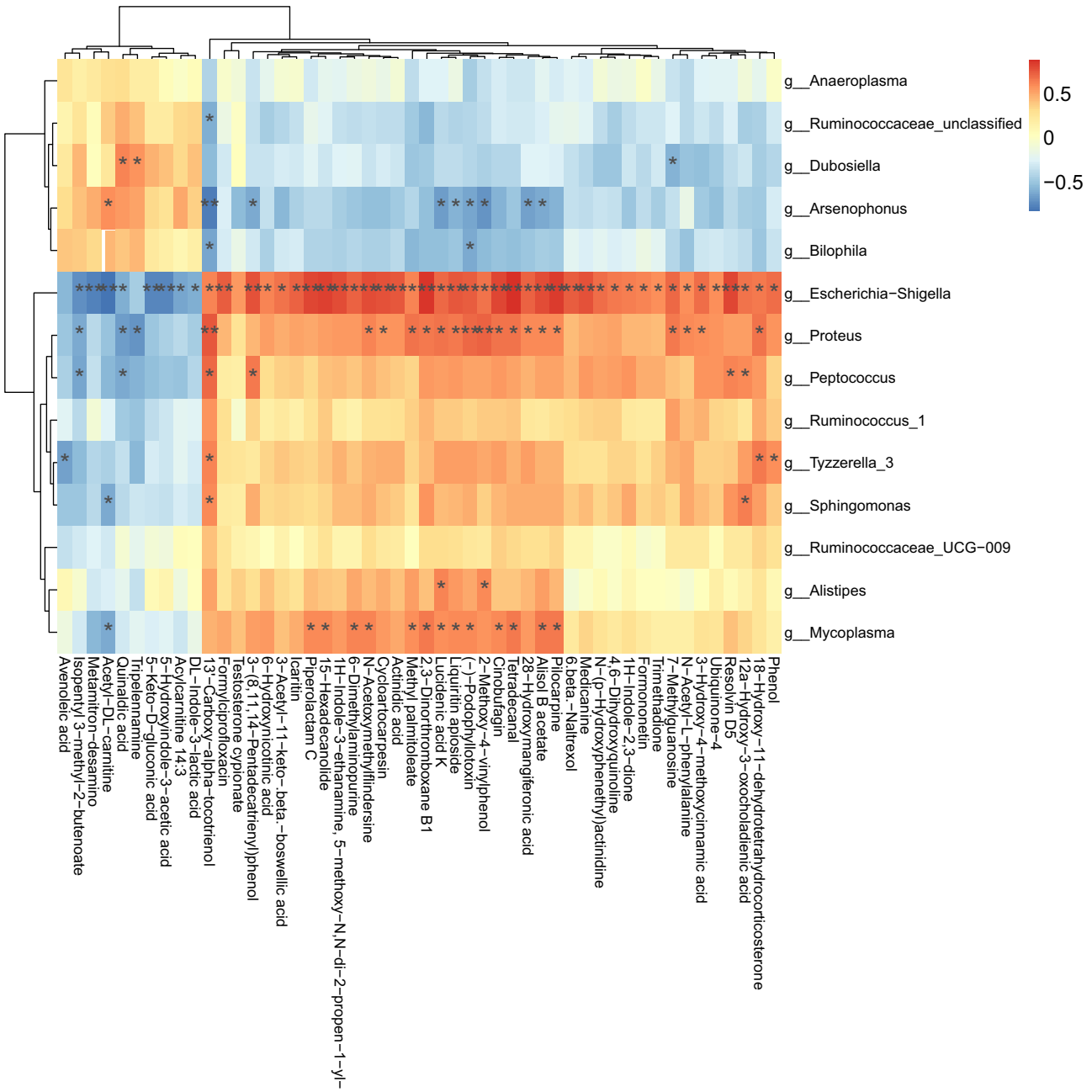

Figure 11 Correlation between gut microbiota and metabolites. **P<0.01; *P<0.05.

confirm that in germ-free mice with induced UC, GCXX treatment was ineffective, further supporting the conclusion that GCXX ameliorated the UC group principally via modulating the gut microbiota.

Discussion

The therapeutic effect of GCXX on UC has been confirmed in previous publications,[38,39] but the actual mechanism remained unclear. In this study, we determined that GCXX was therapeutically effective in the UC mouse model. GCXX improved the symptoms and signs of UC mice, prevented shortening of the colon length and reduced the colonic mucosal and submucosal damage. Additionally, GCXX reduced the levels of serum TNF-α and IT-6, which supported the concept that GCXX had anti-inflammatory effects in the treatment of UC. Moreover, mesalazine, a standard-of-care medication

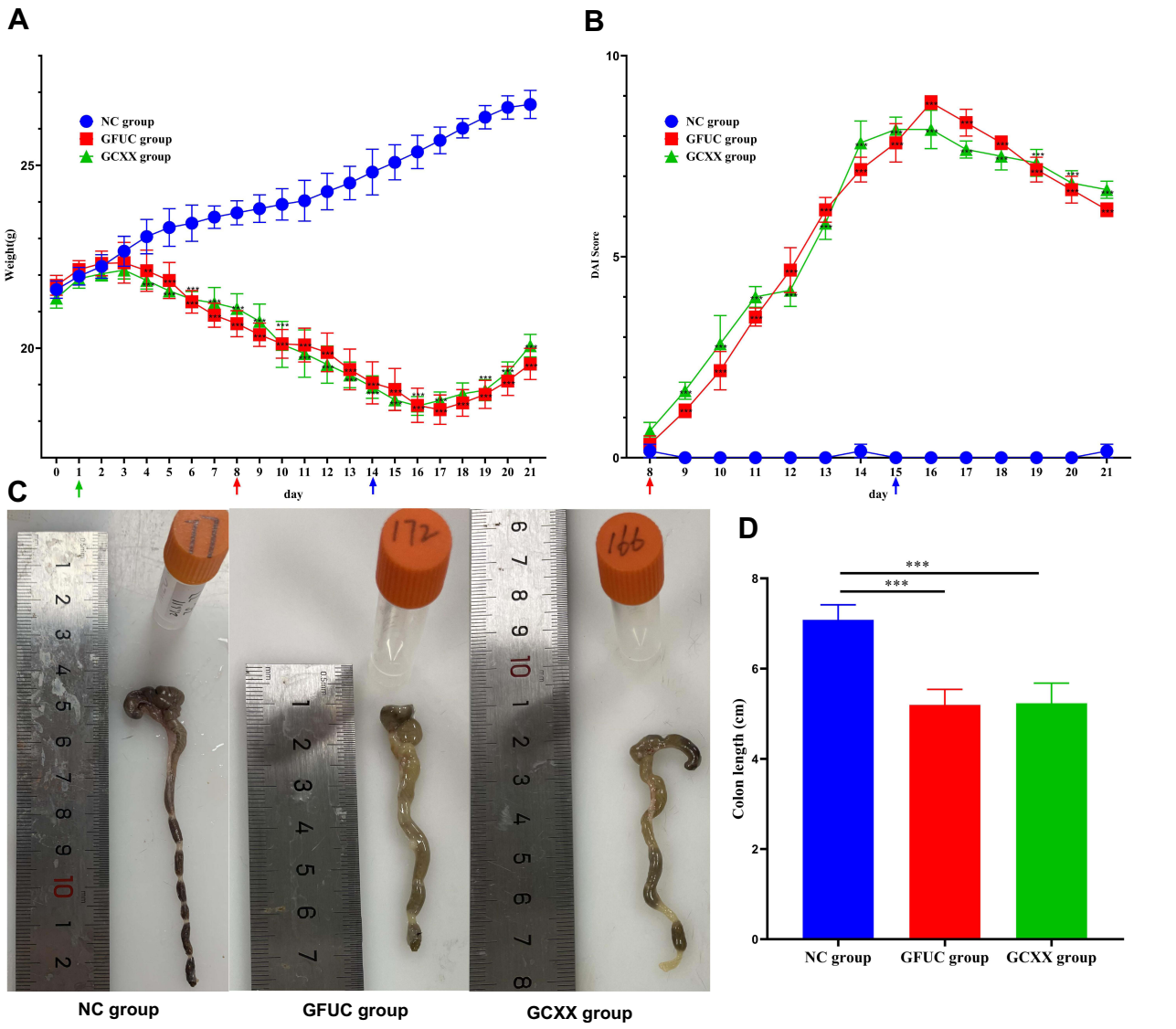

Figure 12 The body weight, DAI score and colon length of mice in each group. (**A**) Changes in body weight of mice throughout the experiment; (**B**) Changes in DAI scores of mice throughout the experiment; (**C**) Typical colon anatomy of mice in each group; (**D**) The colon length of mice in each group. ***P<0.001, **P<0.01, *P<0.05. The green arrow means the first day of inducing germ-free mice, the red arrow means the first day of inducing UC by DSS, and the blue arrow indicates the first day of medication. Compared with the NC group, ***P<0.001, **P<0.01.

prescribed clinically for UC, was used in our study as a comparison for the therapeutic effect of GCXX; the therapeutic effect of GCXX was not statistically different from that of mesalazine.

Although it is generally believed that the etiology of UC is multifactorial, alterations in the gut microbiota and metabolites can contribute significantly to this process.[40] In this study, 16S rDNA high-throughput sequencing technology was utilized to study the effect of GCXX on the gut microbiota of UC mice, and it was significantly disordered. While this appeared initially to manifest as a slight decrease in abundance and diversity, further analysis revealed significant changes in flora structure and function in the UC mice. At the phylum level, the proportion of Proteobacteria was significantly higher than mice in the NC group and the proportion of Patescibacteria was significantly lower. These results illustrated that following induction of UC, the abundance of intestinal pathogenic bacteria increased. A previous report indicated that the gut microbiota composition showed a higher abundance of Proteobacteria in active pancolitis, compared with either patients in remission or healthy participants. Notably, the present study found concordant data that after induction of UC using DSS, the proportion of Proteobacteria was significantly increased.[27,41] Moreover, prior research demonstrated a transiently unstable gut microbiota, especially a Proteobacteria-dominated community could

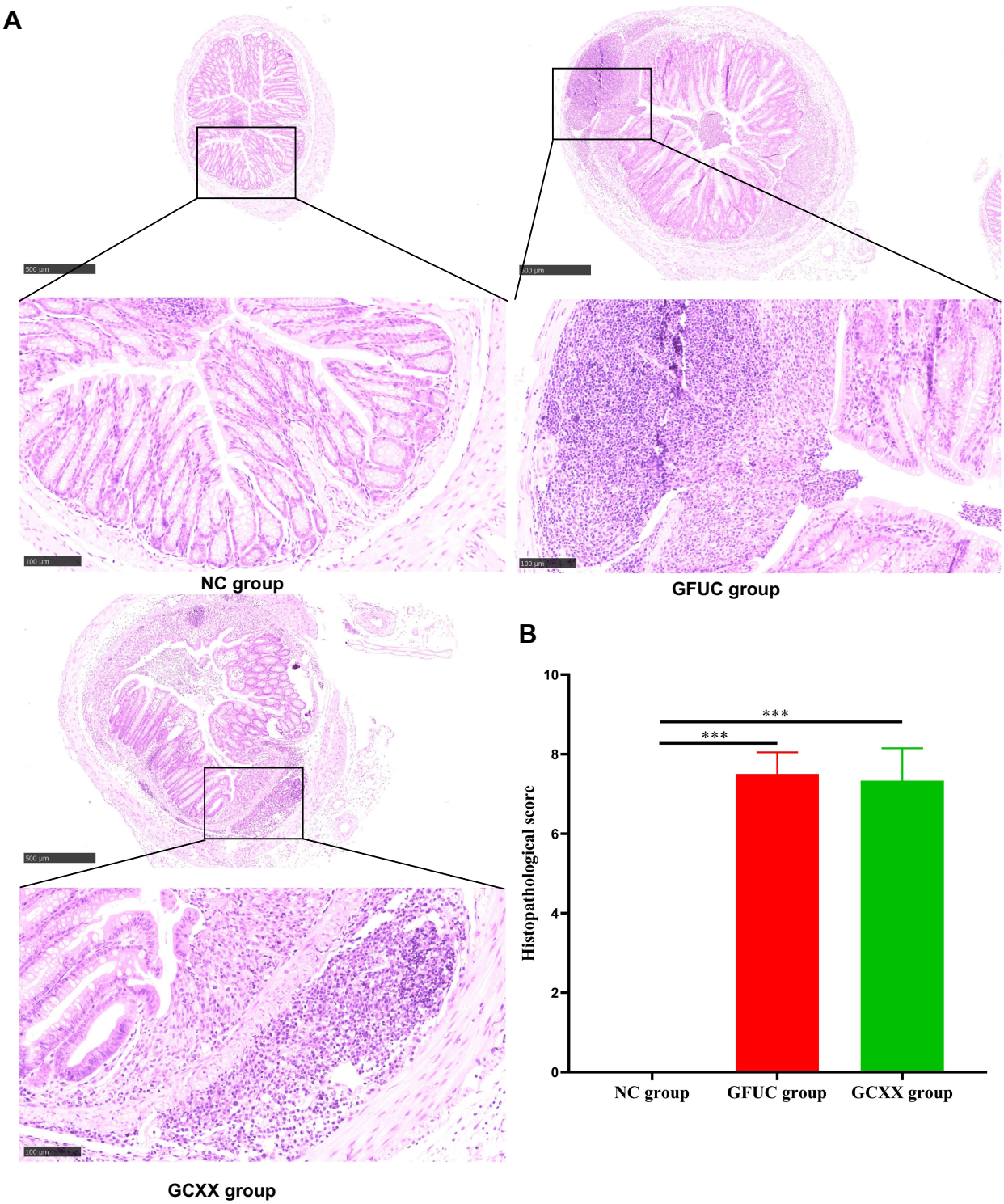

Figure 13 Histopathological changes and scores of colonic tissues of mice in each group. (**A**) Typical histopathological performance of each group (× 5 and × 20). (**B**) Histopathological score of each group. Compared with the NC group, ***P<0.001.

predispose genetically susceptible mice to chronic colitis, as mice lacking Toll-like receptor-5 developed colitis and dysbiosis, which was associated with an abnormal expansion of Proteobacteria.[42] As for Patescibacteria, there were few reports on its role in UC. However, one prior study showed that the proportion of Patescibacteria was increased in mice after DSS-induction of UC,[43] which was not consistent with the results of the present study. Therefore, further

investigation is warranted regarding the role of this bacterium in UC. Turning to Verrucomicrobia (known to contribute to intestinal health), it was proportionately slightly decreased in the UC group when compared to the NC group. This result supported the concept that the proportion of beneficial probiotic bacteria decreased in UC mice. A previous study showed a significant decrease in the phylum Verrucomicrobia in patients with UC,[44] consistent with our study. An anti-inflammatory effect of Verrucomicrobia was previously reported that could reduce the substance triggering colitis.[45] In addition, the quantity of Verrucomicrobia could be decreased due to reduced mucins in patients with UC, which constitute an energy source for this bacteria.[45] After using GCXX, the relative abundance of Proteobacteria slightly decreased and the relative abundance of Patescibacteria and Verrucomicrobia slightly increased, which indicated that GCXX could participate in the regulation of the structure of gut microbiota of UC mice, resulting in the reduction of the level of pathogenic bacteria and an increase in the level of probiotic bacteria. Therefore, we speculated that GCXX might improve the composition of the gut microbiota in UC mice by regulating the relative abundance of Proteobacteria, Patescibacteria, Verrucomicrobia and their subordinate bacteria. At the genus level, the abundance of *Escherichia-Shigella* increased significantly and *Dubosiella* decreased significantly in UC mice. Importantly, following intervention with GCXX, the relative abundance of *Escherichia-Shigella* decreased significantly and *Dubosiella* increased significantly, which indicated that the impact of GCXX regulation principally involved *Escherichia-Shigella* and *Dubosiella*. *Escherichia-Shigella* is a lipopolysaccharide-producing bacteria,[28] which significantly increased in the DSS-induced colitis mice and was associated with intestinal inflammation. It adhered to the mucosal epithelial cells of the colon and destroyed the integrity of the intestinal barrier.[46] Similar findings implicating *Escherichia-Shigella* in UC have been published.[47] Further, *Dubosiella*, recently identified as a novel member of the family Erysipelotrichaceae,[48] was relatively reduced in DSS-induced colitis mice.[43] Previously, *Dubosiell*a was found to play a novel role in regulating SCFA production, and was considered a SCFA producing bacteria.[49] Therefore, the ameliorative effect of GCXX on DSS-induced colitis was likely achieved in part by reducing the abundance of the classic pathogen *Escherichia-Shigella* and increasing the relative abundance of the novel probiotic *Dubosiell*a. Hence, restoration of the appropriate balance of *Escherichia-Shigella* and *Dubosiell*a contributed to the reestablishment of intestinal equilibrium due to GCXX treatment.

To analyze the metabolite profiles derived from gut microbiota, particularly to monitor and capture potential metabolic responses and biomarkers, we used UPLC-Q-TOF-MS-based untargeted metabolomics. The results indicated that most of the differential abundant metabolites were organic acids and derivatives, lipids and lipid-like molecules, and organoheterocyclic compounds. Following induction of UC by DSS, the level of acetic acid significantly decreased, concordant with prior literature.[50] Acetic acid, a SCFA that is produced by gut microbiota, takes part in maintaining the intestinal function, morphology and function of colonic epithelial cells.[51] In our study, acetic acid increased slightly after treatment with GCXX, but this change was not significant. Compared with the NC group, linoleic acid was significantly higher in the UC group, and decreased following intervention with GCXX. Linoleic acid, as a precursor of arachidonic acid synthesis, plays an important role in the development of inflammation,[52,53] and the linoleic acid metabolic pathway was previously reported to be the most influential metabolic pathway in UC.[54] The metabolism of linoleic acid might be related to Proteobacteria,[55] which was consistent with the results of the gut microbiota in the present study. Namely, GCXX was found to reduce the level of linoleic acid and exert an anti-inflammatory effect in the development of UC. Moreover, GCXX was demonstrated to partially regulate the metabolism of amino acids; the levels of L-tyrosine, tyrosine, serine and L-serine decreased in UC mice, but increased slightly following treatment with GCXX, although the levels did not fully return to normal. A prior study reported that L-tyrosine, a non-essential amino acid, was negatively related to Proteus in DSS-induced colitis mice,[56] which indicated that L-tyrosine might alleviate UC. Moreover, serine was reportedly able to prevent inflammation and improve intestinal integrity and gut microbiota composition in DSS-induced colitis mice; L-serine also had an anti-inflammatory effect on LPS-treated mice.[57] Therefore, we speculated that GCXX might ameliorate UC by regulating the above-mentioned amino acids.

In the process of metabolite detection, a significant difference in linolenic acid between the UC and GCXX groups was detected, and subsequently determined that GCXX could regulate the linolenic acid metabolism pathway. Moreover, we found that GCXX could regulate tryptophan metabolism. A prior study analyzed serum samples from more than 500 patients with IBD, and found a negative correlation between tryptophan and disease activity that was interpreted to suggest that tryptophan deficiency could contribute to the development of IBD.[58] Studies also showed that tryptophan

could protect from inflammation by maintaining gut immune homeostasis and microbial diversity in DSS-induced colitis mice.[59,60] In experimental colitis models, tryptophan-deficient mice showed aggravation of colitis,[61] and addition of tryptophan to a normal diet could reduce the symptoms of DSS-induced colitis, improve histology and intestinal permeability.[62] Moreover, additional studies have reported that because gut microbiota metabolize tryptophan to indole derivates, these could induce local production of IL-22,[63] which would maintain intestinal homeostasis and promote immune defense and tissue repair.[61–63] In the present study, GCXX was found to regulate the metabolism of tryptophan, and multiple indoles and derivatives were detected, including indole, indole-3-carboxyaldehyde, 5-hydroxyindole-3-acetic acid, 3-formyl-6-hydroxyindole, 1H-indole-2,3-dione and 1H-indole-3-carboxaldehyde. These metabolites were diminished in the DSS-induced colitis mice, but then increased following treatment with GCXX. Aggregating the prior published work together with our findings strongly indicated that GCXX had a regulatory function in the metabolism of tryptophan and of indoles and derivatives that could play a significant role in the treatment of UC.

Finally, because GCXX did not ameliorate DSS-induced colitis in germ-free mice, these results provided further evidence that the mechanism by which GCXX ameliorated UC was mainly through modulation of the gut microbiota and metabolites.

Conclusion

Our study demonstrated that GCXX intervention could ameliorate DSS-induced colonic damage and reduce colonic inflammation. These therapeutic effects seemed to result from GCXX restoring the structure and function of the gut microbiota and modifying its metabolic profiling. Specifically, the results of 16S rDNA high-throughput gene sequencing showed that GCXX could alter the composition of gut microbiota by proportionately increasing *Dubosiella* and decreasing *Escherichia-Shigella*. Untargeted metabolomics showed that GCXX could change the content of certain metabolites such as linoleic acid and some amino acids, even participating in the pathway regulation of linoleic acid and amino acid metabolism. Overall, our research helped to clarify the mechanism of GCXX in the treatment of UC which could serve as an important basis of reference for further study.

Abbreviations

UC, ulcerative colitis; IBD, inflammatory bowel diseases; SCFAs, short chain fatty acids; IL-18, interleukin-18; IL-6, interleukin-6; IL-17, interleukin-17; TNF-α, tumour necrosis factor-α; TCM, traditional Chinese medicine; GCXX, Gancao Xiexin decoction; RT-PCR, real-time polymerase chain reactions; DSS, dextran sulfate sodium; DAI, disease activity index; UPLC-Q-TOF-MS, ultra-performance liquid chromatography combined with quadrupole time-of-flight mass spectrometry; IS, internal standard; SPF, specific-pathogen-free; NC group, normal-control group; UC group, UC model group; GCXX group, GCXX treatment group; Mes group, mesalazine treatment group; GMes group, GCXX combined with mesalazine treatment group; H&E, Hematoxylin and Eosin; ELISA, Enzyme-linked immunosorbent assay; LC-MS, liquid chromatography combined with mass spectrometry; QC, Quality Control; MS, mass spectrometry; PSI, per square inch; IDA, information-dependent acquisition; TDC, target-decoy competition; PLS-DA, Partial Least Squares Discriminant Analysis; VIP, variable importance in the projection; SD, standard deviation; GFUC group, germ-free UC model group; OTUs, observed operational taxonomic units; PCoA, principal coordinate analysis; LEfSe, the linear discriminant analysis effect size; LDA, Linear discriminant analysis; TICs, Total ion chromatograms; PCA, Principal component analysis; OPLS-DA, orthogonal partial least squares discriminant analysis; KEGG, Kyoto Encyclopedia of Genes and Genomes.

Ethical Approval

The experimental procedures were reviewed and approved by the Committee for the Care and Use of Laboratory Animals at Zhejiang Chinese Medical University (Hangzhou, Zhejiang, China).

Acknowledgments

This research was supported by Zhejiang Traditional Chinese Medicine Administration (No: 2020ZZ010). The authors would like to express their gratitude to EditSprings (https://www.editsprings.cn) for the expert linguistic services provided.

Disclosure

The authors report no conflicts of interest in this work.

References

1. Kobayashi T, Siegmund B, Le Berre C, et al. Ulcerative colitis. *Nat Rev Dis Primers*. 2020;6(1):74.
2. Ungaro R, Mehandru S, Allen PB, Peyrin-Biroulet L, Colombel JF. Ulcerative colitis. *Lancet*. 2017;389(10080):1756–1770.
3. Yadav V, Varum F, Bravo R, Furrer E, Bojic D, Basit AW. Inflammatory bowel disease: exploring gut pathophysiology for novel therapeutic targets. *Transl Res*. 2016;176:38–68.
4. Park JH, Peyrin-Biroulet L, Eisenhut M, Shin JI. IBD immunopathogenesis: a comprehensive review of inflammatory molecules. *Autoimmun Rev*. 2017;16(4):416–426.
5. Du L, Ha C. Epidemiology and Pathogenesis of Ulcerative Colitis. *Gastroenterol Clin North Am*. 2020;49(4):643–654.
6. Garg M, Hendy P, Ding JN, Shaw S, Hold G, Hart A. The Effect of Vitamin D on Intestinal Inflammation and Faecal Microbiota in Patients with Ulcerative Colitis. *J Crohns Colitis*. 2018;12(8):963–972.
7. Shen ZH, Zhu CX, Quan YS, et al. Relationship between intestinal microbiota and ulcerative colitis: mechanisms and clinical application of probiotics and fecal microbiota transplantation. *World J Gastroenterol*. 2018;24(1):5–14.
8. Nishida A, Inoue R, Inatomi O, Bamba S, Naito Y, Andoh A. Gut microbiota in the pathogenesis of inflammatory bowel disease. *Clin J Gastroenterol*. 2018;11(1):1–10.
9. Sun M, Wu W, Liu Z, Cong Y. Microbiota metabolite short chain fatty acids, GPCR, and inflammatory bowel diseases. *J Gastroenterol*. 2017;52(1):1–8.
10. Parada Venegas D, De la Fuente MK, Landskron G, et al. Short Chain Fatty Acids (SCFAs)-Mediated Gut Epithelial and Immune Regulation and Its Relevance for Inflammatory Bowel Diseases. *Front Immunol*. 2019;10:277.
11. Fukuda S, Toh H, Hase K, et al. Bifidobacteria can protect from enteropathogenic infection through production of acetate. *Nature*. 2011;469 (7331):543–547.
12. den Besten G, van Eunen K, Groen AK, Venema K, Reijngoud DJ, Bakker BM. The role of short-chain fatty acids in the interplay between diet, gut microbiota, and host energy metabolism. *J Lipid Res*. 2013;54(9):2325–2340.
13. Collins J, Robinson C, Danhof H, et al. Dietary trehalose enhances virulence of epidemic Clostridium difficile. *Nature*. 2018;553(7688):291–294.
14. Ng SC, Shi HY, Hamidi N, et al. Worldwide incidence and prevalence of inflammatory bowel disease in the 21st century: a systematic review of population-based studies. *Lancet*. 2017;390(10114):2769–2778.
15. Ananthakrishnan AN, Kaplan GG, Ng SC. Changing Global Epidemiology of Inflammatory Bowel Diseases: sustaining Health Care Delivery Into the 21st Century. *Clin Gastroenterol Hepatol*. 2020;18(6):1252–1260.
16. Benchimol EI, Mack DR, Guttmann A, et al. Inflammatory bowel disease in immigrants to Canada and their children: a population-based cohort study. *Am J Gastroenterol*. 2015;110(4):553–563.
17. Ng SC, Kaplan GG, Tang W, et al. Population Density and Risk of Inflammatory Bowel Disease: a Prospective Population-Based Study in 13 Countries or Regions in Asia-Pacific. *Am J Gastroenterol*. 2019;114(1):107–115.
18. Kotze PG, Underwood FE, Damião AOMC, et al. Progression of Inflammatory Bowel Diseases Throughout Latin America and the Caribbean: a Systematic Review. *Clin Gastroenterol Hepatol*. 2020;18(2):304–312.
19. Parente JM, Coy CS, Campelo V, et al. Inflammatory bowel disease in an underdeveloped region of Northeastern Brazil. *World J Gastroenterol*. 2015;21(4):1197–1206.
20. Panés J, Alfaro I. New treatment strategies for ulcerative colitis. *Expert Rev Clin Immunol*. 2017;13(10):963–973.
21. Frias Gomes C, Chapman TP, Satsangi J. De-escalation of medical therapy in inflammatory bowel disease. *Curr Opin Pharmacol*. 2020;55:73–81.
22. Troncone E, Monteleone G. The safety of non-biological treatments in Ulcerative Colitis. *Expert Opin Drug Saf*. 2017;16(7):779–789.
23. Liu YX. Application of Zhang Zhongjing Gancao Xiexin Decoction. *Zhejiang J Tradit Chin Med*. 2012;47(9):653–654.
24. Chang Y, Li YL. Observation on Curative Effect of Modified Gancaoxiexin Decoction on Peptic Ulcer. *J Emerg Tradit Chin Med*. 2014;23(6):1145–1146.
25. Sun YW, Zhang L. Effect of liquorice decoction combined with mesalazine on serum inflammatory factors and T lymphocyte levels in patients with ulcerative colitis. *World Chin J Digestol*. 2018;26(32):1879–1885.
26. Shen LN, Liu J, Qian YD, Xiong L. Efficacy of Gancao Xiexin Decoction combined with mesalazine on patients with ulcerative colitis and the influence of intestinal flora and serum inflammatory factors. *Chin J Integr Tradit West Med*. 2021;29(7):474–478.
27. Cui L, Guan X, Ding W, et al. Scutellaria baicalensis Georgi polysaccharide ameliorates DSS-induced ulcerative colitis by improving intestinal barrier function and modulating gut microbiota. *Int J Biol Macromol*. 2021;166:1035–1045.
28. Peng L, Gao X, Nie L, et al. Astragalin Attenuates Dextran Sulfate Sodium (DSS)-Induced Acute Experimental Colitis by Alleviating Gut Microbiota Dysbiosis and Inhibiting NF-κB Activation in Mice. *Front Immunol*. 2020;11:2058.
29. Chen XQ, Lv XY, Liu SJ. Baitouweng decoction alleviates dextran sulfate sodium-induced ulcerative colitis by regulating intestinal microbiota and the IL-6/STAT3 signaling pathway. *J Ethnopharmacol*. 2021;265:113357.
30. Chen DX. *The Formulaology of TCM*. Beijing: Qinghua university press; 2013.
31. Wang L, Qiu XM, Gui YY, Xu YP, Gober HJ, Li DJ. Bu-Shen-Ning-Xin Decoction ameliorated the osteoporotic phenotype of ovariectomized mice without affecting the serum estrogen concentration or uterus. *Drug Des Devel Ther*. 2015;9:5019–5031.
32. Xuan C, Xi YM, Zhang YD, Tao CH, Zhang LY, Cao WF. Yiqi Jiedu Huayu Decoction Alleviates Renal Injury in Rats With Diabetic Nephropathy by Promoting Autophagy. *Front Pharmacol*. 2021;12:624404.
33. Liu K, Jia B, Zhou L, et al. Ultraperformance Liquid Chromatography Coupled with Quadrupole Time-of-Flight Mass Spectrometry-Based Metabolomics and Lipidomics Identify Biomarkers for Efficacy Evaluation of Mesalazine in a Dextran Sulfate Sodium-Induced Ulcerative Colitis Mouse Model. *J Proteome Res*. 2021;20(2):1371–1381.
34. Li MY, Luo HJ, Wu X, et al. Anti-Inflammatory Effects of Huangqin Decoction on Dextran Sulfate Sodium-Induced Ulcerative Colitis in Mice Through Regulation of the Gut Microbiota and Suppression of the Ras-PI3K-Akt-HIF-1α and NF-κB Pathways. *Front Pharmacol*. 2020;10:1552.
35. Yuan Z, Yang L, Zhang X, Ji P, Wei Y. Therapeutic effect of n-butanol fraction of Huang-lian-Jie-du Decoction on ulcerative colitis and its regulation on intestinal flora in colitis mice. *Biomed Pharmacother*. 2020;121:109638.

36. Wu ZC, Zhao ZL, Deng JP, Huang JT, Wang YF, Wang ZP. Sanhuang Shu'ai decoction alleviates DSS-induced ulcerative colitis via regulation of gut microbiota, inflammatory mediators and cytokines. *Biomed Pharmacother*. 2020;125:109934.
37. Wu J, Wei Z, Cheng P, et al. Rhein modulates host purine metabolism in intestine through gut microbiota and ameliorates experimental colitis. *Theranostics*. 2020;10(23):10665–10679.
38. Li EL, Zhao Y. Analysis of Clinical Effect of Modified Gancaoxiexin Decoction on Patients with Ulcerative Colitis. *China Foreign Me*. 2020;39 (31):178–180.
39. Ma YM. Therapeutic effect and research of Gancao Xiexin Decoction on ulcerative colitis. *Dietetics*. 2019;4:70.
40. Franzosa EA, Sirota-Madi A, Avila-Pacheco J, et al. Gut microbiome structure and metabolic activity in inflammatory bowel disease. *Nat Microbiol*. 2019;4:293–305.
41. Maldonado-Arriaga B, Sandoval-Jiménez S, Rodríguez-Silverio J, et al. Gut dysbiosis and clinical phases of pancolitis in patients with ulcerative colitis. *Microbiologyopen*. 2021;10(2):e1181.
42. Carvalho FA, Koren O, Goodrich JK, et al. Transient inability to manage proteobacteria promotes chronic gut inflammation in TLR5-deficient mice. *Cell Host Microbe*. 2012;12(2):139–152.
43. Chen J, Zhang LK, Gu WC, et al. Effect of Banxia Xiexin Decoction on intestinal flora of mice with ulcerative colitis induced by dextran sodium sulfate. *Chin J Chin Mater Med*. 2021;46(11):2871–2880.
44. Shah R, Cope JL, Nagy-Szakal D, et al. Composition and function of the pediatric colonic mucosal microbiome in untreated patients with ulcerative colitis. *Gut Microbes*. 2016;7(5):384–396.
45. Kang CS, Ban M, Choi EJ, et al. Extracellular vesicles derived from gut microbiota, especially Akkermansia muciniphila, protect the progression of dextran sulfate sodium-induced colitis. *PLoS One*. 2013;8(10):e76520.
46. Chen L, Wang W, Zhou R, et al. Characteristics of fecal and mucosa-associated microbiota in Chinese patients with inflammatory bowel disease. *Medicine (Baltimore)*. 2014;93(8):e51.
47. Xu J, Chen N, Wu Z, et al. 5-Aminosalicylic Acid Alters the Gut Bacterial Microbiota in Patients With Ulcerative Colitis. *Front Microbiol*. 2018;9:1274.
48. Cox LM, Sohn J, Tyrrell KL, et al. Description of two novel members of the family Erysipelotrichaceae: ileibacterium valens gen. nov., sp. nov. and Dubosiella newyorkensis, gen. nov., sp. nov., from the murine intestine, and emendation to the description of Faecalibaculum rodentium. *Int J Syst Evol Microbiol*. 2017;67(10):1247–1254.
49. Ai X, Wu C, Yin T, et al. Antidiabetic Function of Lactobacillus fermentum MF423-Fermented Rice Bran and Its Effect on Gut Microbiota Structure in Type 2 Diabetic Mice. *Front Microbiol*. 2021;12:682290.
50. Kim CH, Park J, Kim M. Gut microbiota-derived short-chain Fatty acids, T cells, and inflammation. *Immune Netw*. 2014;14(6):277–288.
51. Koh A, De Vadder F, Kovatcheva-Datchary P, Bäckhed F. From Dietary Fiber to Host Physiology: short-Chain Fatty Acids as Key Bacterial Metabolites. *Cell*. 2016;165(6):1332–1345.
52. Ramsden CE, Ringel A, Feldstein AE, et al. Lowering dietary linoleic acid reduces bioactive oxidized linoleic acid metabolites in humans. *Prostaglandins Leukot Essent Fatty Acids*. 2012;87(4–5):135–141.
53. Zhang W, Chen Y, Jiang H, et al. Integrated strategy for accurately screening biomarkers based on metabolomics coupled with network pharmacology. *Talanta*. 2020;211:120710.
54. Tang Q, Cang S, Jiao J, et al. Integrated study of metabolomics and gut metabolic activity from ulcerative colitis to colorectal cancer: the combined action of disordered gut microbiota and linoleic acid metabolic pathway might fuel cancer. *J Chromatogr A*. 2020;1629:461503.
55. Lozupone CA, Stombaugh JI, Gordon JI, Jansson JK, Knight R. Diversity, stability and resilience of the human gut microbiota. *Nature*. 2012;489 (7415):220–230.
56. Ren J, Li P, Yan D, et al. Interplay between the gut microbiome and metabolism in ulcerative colitis mice treated with the dietary ingredient phloretin. *J Microbiol Biotechnol*. 2021;31:10.
57. Zhang H, Hua R, Zhang B, Zhang X, Yang H, Zhou X. Serine Alleviates Dextran Sulfate Sodium-Induced Colitis and Regulates the Gut Microbiota in Mice. *Front Microbiol*. 2018;9:3062.
58. Nikolaus S, Schulte B, Al-Massad N, et al. Increased Tryptophan Metabolism Is Associated With Activity of Inflammatory Bowel Diseases. *Gastroenterology*. 2017;153(6):1504–1516.e2.
59. Zelante T, Iannitti RG, Cunha C, et al. Tryptophan catabolites from microbiota engage aryl hydrocarbon receptor and balance mucosal reactivity via interleukin-22. *Immunity*. 2013;39(2):372–385.
60. Lamas B, Richard ML, Leducq V, et al. CARD9 impacts colitis by altering gut microbiota metabolism of tryptophan into aryl hydrocarbon receptor ligands. *Nat Med*. 2016;22(6):598–605.
61. Hashimoto T, Perlot T, Rehman A, et al. ACE2 links amino acid malnutrition to microbial ecology and intestinal inflammation. *Nature*. 2012;487 (7408):477–481.
62. Kim CJ, Kovacs-Nolan JA, Yang C, Archbold T, Fan MZ, Mine Y. l-Tryptophan exhibits therapeutic function in a porcine model of dextran sodium sulfate (DSS)-induced colitis. *J Nutr Biochem*. 2010;21(6):468–475.
63. Jin UH, Lee SO, Sridharan G, et al. Microbiome-derived tryptophan metabolites and their aryl hydrocarbon receptor-dependent agonist and antagonist activities. *Mol Pharmacol*. 2014;85(5):777–788.